Electronic Supplementary Material (ESI) for Catalysis Science & Technology.

Asymmetric hydroamination with far fewer chiral species than copper centres achieved by tuning the structure of supramolecular helical benzene-1,3,5-tricarboxamide based catalysts

Paméla Aoun, Ahmad Hammoud, Mayte A. Martínez-Aguirre, Laurent Bouteiller, and Matthieu Raynal*

Supplementary Charts, Figures and Tables (Chart S1, Figures S1-S12, Tables S1-S3) _____ *2*

Preparation of the solutions _____ *21*

Material and methods _____ *25*

Synthesis of BTA ligands _____ *28*

Selected ^{1}H NMR, MS and chiral HPLC analyses of catalytic samples _____ *33*

NMR spectra _____ *48*

References _____ *54*

Supplementary Charts, Figures and Tables (Chart S1, Figures S1-S12, Tables S1-S3)

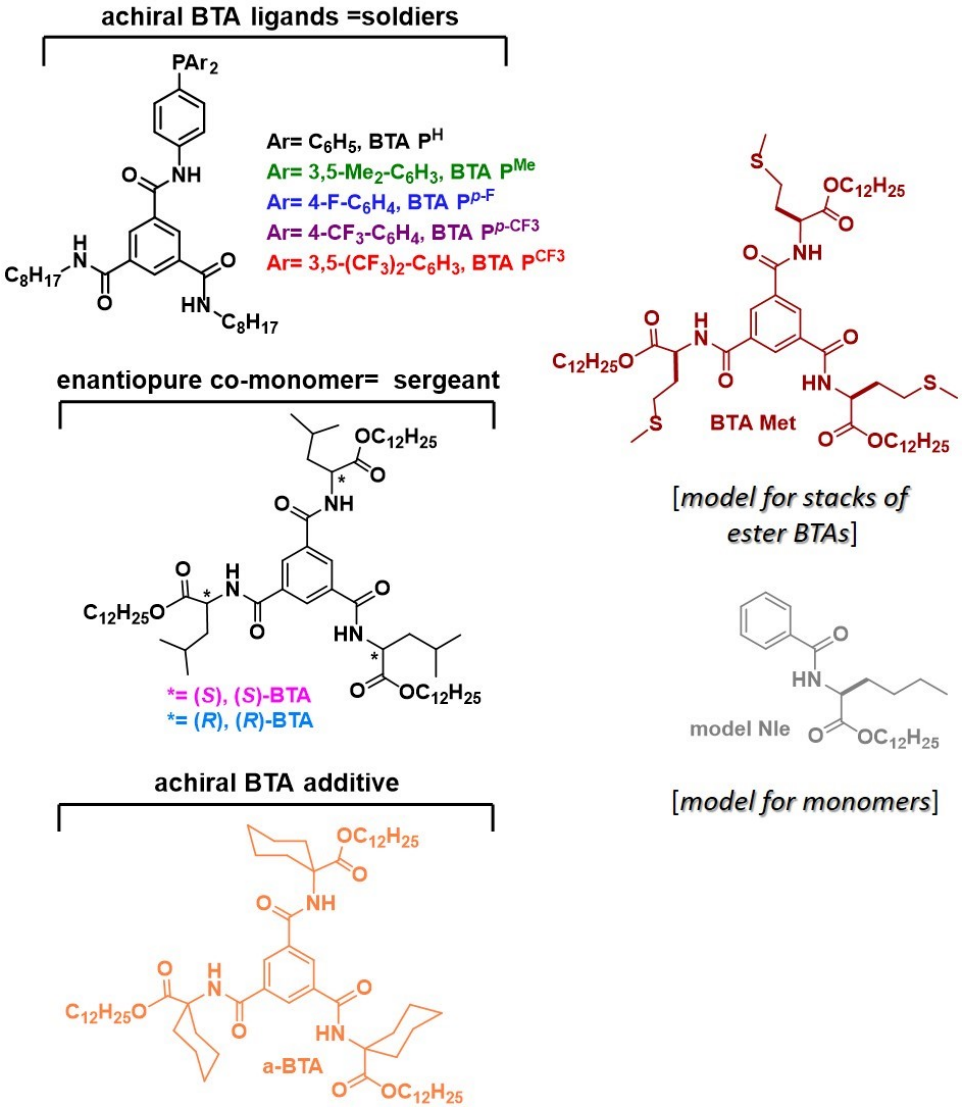

Chart S1 Chemical structures of the BTA monomers employed in this study as well as **BTA Met** and **model Nle** (models for the spectroscopic signature of ester BTA in stacks and monomers, respectively).[1]

General formulas:

$$\text{fs0} = \text{fraction of sergeant introduced into the solution} = \frac{[(\boldsymbol{R})\textbf{ - BTA}]0}{[(\boldsymbol{R})\textbf{ - BTA}]0 + [\textbf{BTA ligand}]0 + [\textbf{a - BTA}]0}$$

$$\text{fss} = \text{fraction of sergeant in stacks} = \frac{[(\boldsymbol{R})\textbf{ - BTA in stacks}]}{[(\boldsymbol{R})\textbf{ - BTA in stacks}] + [\textbf{BTA ligand}]0 + [\textbf{a - BTA}]0}$$

$[(\boldsymbol{R})\textbf{ - BTA}]$ in stacks is determined by FT - IR or SANS analyses

$$\text{BTA in stacks (molar fraction)} = \frac{[(\boldsymbol{R})\textbf{ - BTA in stacks}] + [\textbf{BTA ligand}]0 + [\textbf{a - BTA}]0}{[(\boldsymbol{R})\textbf{ - BTA}]0 + [\textbf{BTA ligand}]0 + [\textbf{a - BTA}]0}$$

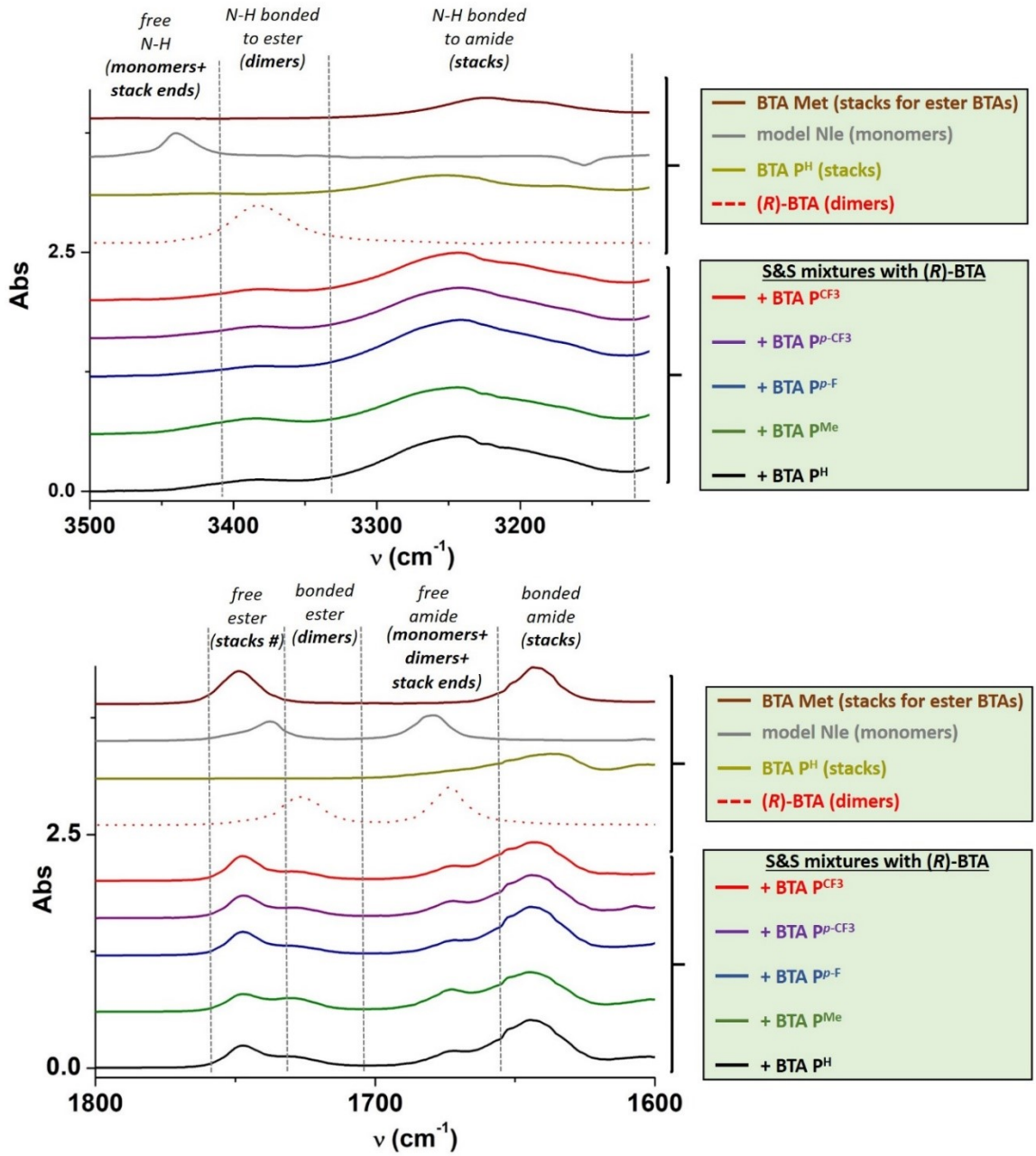

Figure S1 FT-IR analyses of individual components **(*R*)-BTA** (3.11 mM), **BTA P^{H}** (4.82 mM), **model Nle** (10 mM), **BTA Met** (10 mM) and of the S&S-type mixtures **BTAP^{H}** (4.82 mM)/**(*R*)-BTA** (3.11 mM, f_s^0=39%), **BTAP^{Me}** (4.45 mM)/**(*R*)-BTA** (3.11 mM, f_s^0=41%), **BTA P$^{p\text{-}F}$** (4.58 mM)/**(*R*)-BTA** (3.11 mM, f_s^0=41%), **BTA P$^{p\text{-}CF3}$** (4.02 mM)/**(*R*)-BTA** (3.11 mM, f_s^0=44%), and **BTA P^{CF3}** (3.45 mM)/**(*R*)-BTA** (3.11 mM, f_s^0=47%) in toluene-d_8 (except for **BTA Met** and **model Nle** in cyclohexane) at 293 K. Zoom on the N−H, ester carbonyl and amide I carbonyl regions. The intensity of the spectra in the N−H region is multiplied five times, except for **model Nle** (× 10), **BTA Met** (× 2.5) and **BTA P^{H}** (× 2.5). The nature of the different stretching frequencies are assigned according to literature.[1,2]

free ester C=O bands are also seen for ester BTAs in the monomer state (see **model Nle**) but these species are not expected to be present in the S&S mixtures since **(*R*)-BTA** exists under the form of dimers or stacks under these conditions.[1,2]

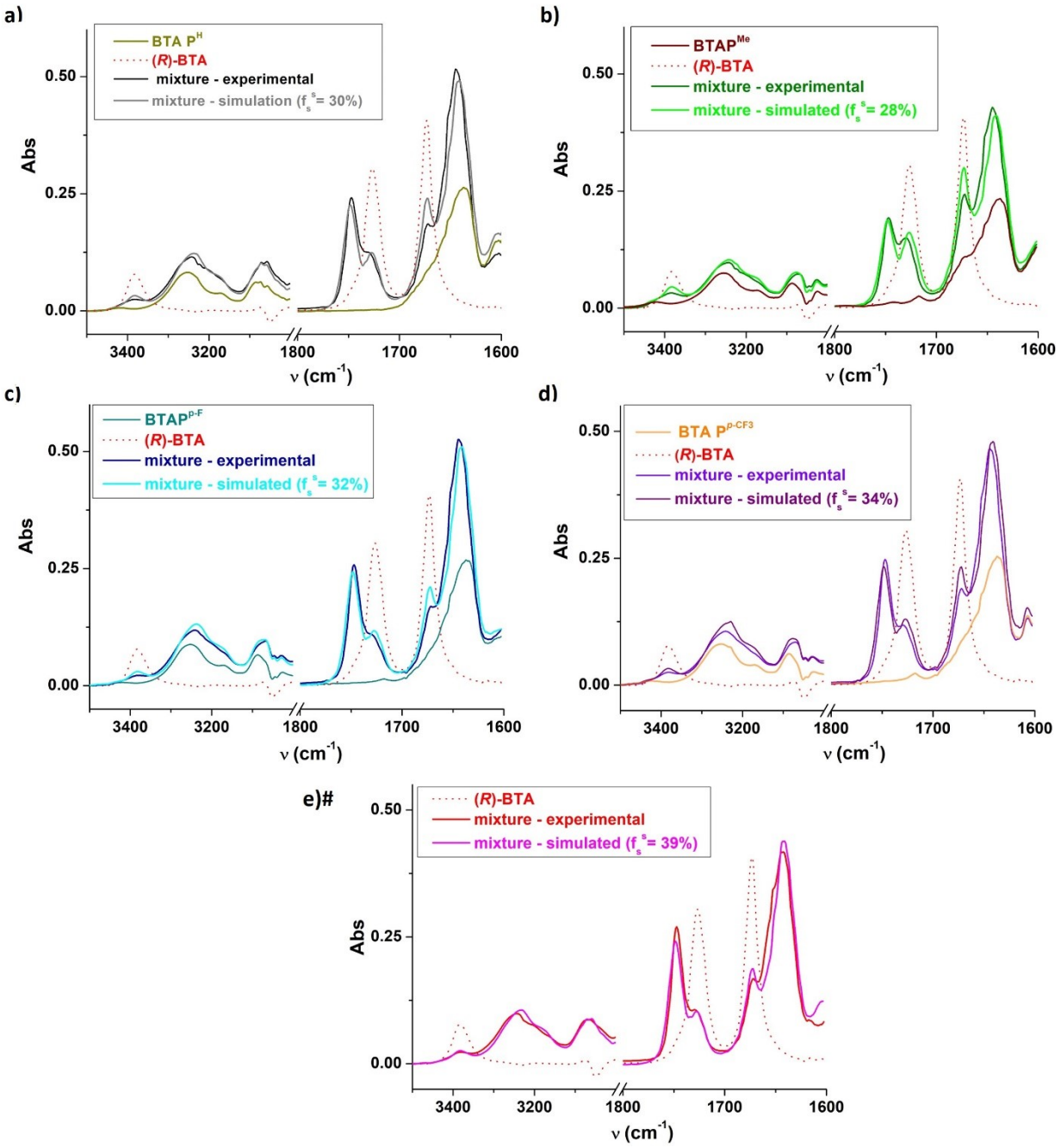

Figure S2 Comparison between experimental and simulated FT-IR spectra for the different S&S-type mixtures between **(*R*)-BTA** and **BTA P^{H}** (a), **BTAP^{Me}** (b), **BTA P$^{p\text{-}F}$** (c), **BTA P$^{p\text{-}CF3}$** (d) and **BTA P^{CF3}** (e) (same conditions than those indicated in Figure S1). The experimental and simulated FT-IR spectra are shown together with those of pure BTA ligand and pure **(*R*)-BTA**.# The FT-IR spectra of the mixtures were simulated considering that a fraction of sergeant (f_s^s-IR, obtained by fitting the bands in the ester C=O region) is incorporated into the stacks of the BTA ligand (see the full description of the procedure in the Material and Methods part).

FT-IR analysis of **BTA P^{CF3}** alone was precluded by its limited solubility.

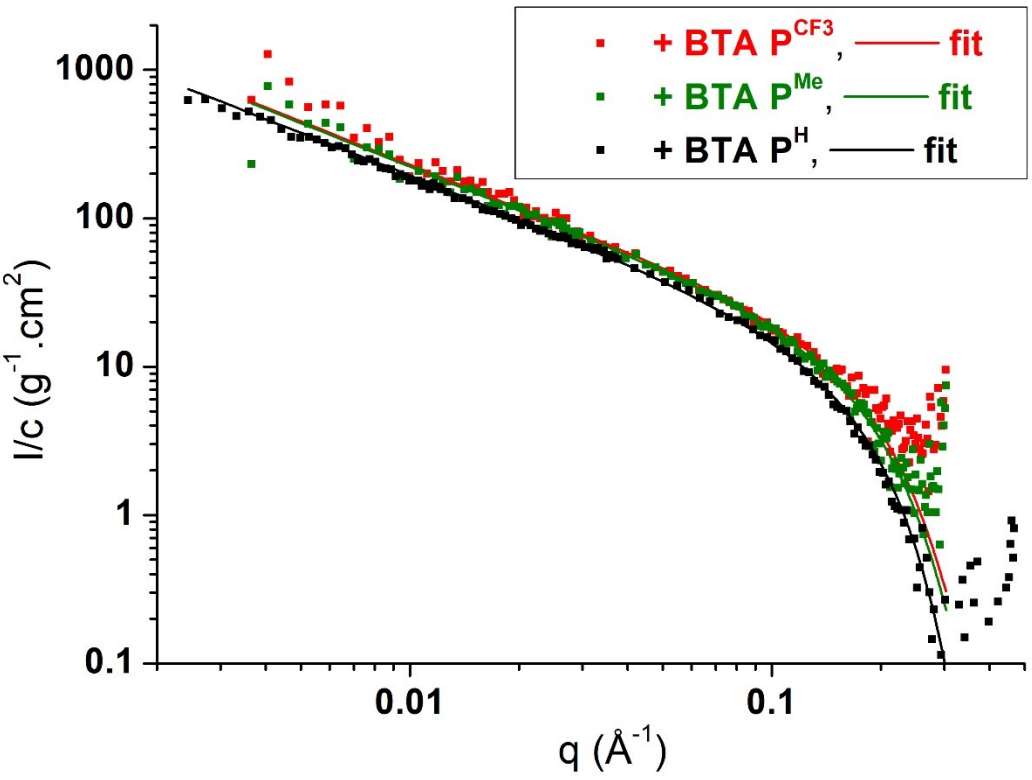

Figure S3 SANS analyses: scattered intensity (cm^{-1}) normalized by the (total BTA) concentration for the S&S-type mixtures containing **BTA P^{H}** (5.78 mM)/**(*R*)-BTA** (3.72 mM, f_s^0= 39%), **BTA P^{Me}** (4.46 mM)/**(*R*)-BTA** (3.11 mM, f_s^0= 41%), and **BTA P^{CF3}** (3.45 mM)/**(*R*)-BTA** (3.11 mM, f_s^0= 47%) in toluene-d_8.

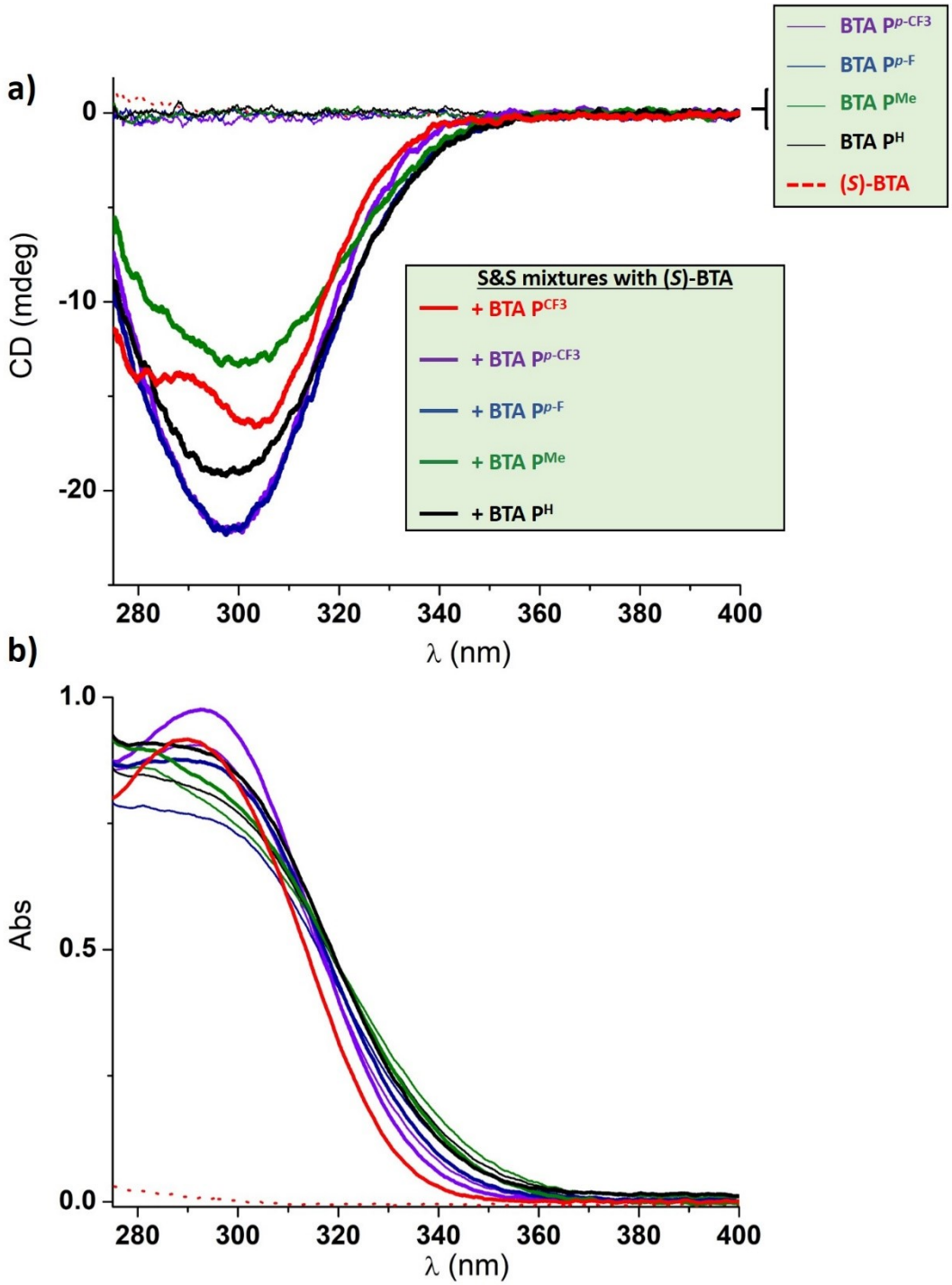

Figure S4 CD (a) and UV-Vis (b) analyses of pure **(*S*)-BTA** (3.11 mM) and BTA ligands (3.33 g.L^{-1}) and of the S&S-type mixtures **BTA P^{H}** (4.82 mM)/**(*S*)-BTA** (3.11 mM, f_s^0=39%), **BTA P^{Me}** (4.45 mM)/**(*S*)-BTA** (3.11 mM, f_s^0=41%), **BTA P$^{p\text{-}F}$** (4.58 mM)/**(*S*)-BTA** (3.11 mM, f_s^0=41%), **BTA P$^{p\text{-}CF3}$** (4.02 mM)/**(*S*)-BTA** (3.11 mM, f_s^0=44%), and **BTA P^{CF3}** (3.45 mM)/**(*S*)-BTA** (3.11 mM, f_s^0=47%) in toluene-d_8 at 293 K. The observed CD signals belong to BTA ligands only and are thus ICD signals[3] which reflect the chiral environment of the ligands.[4]

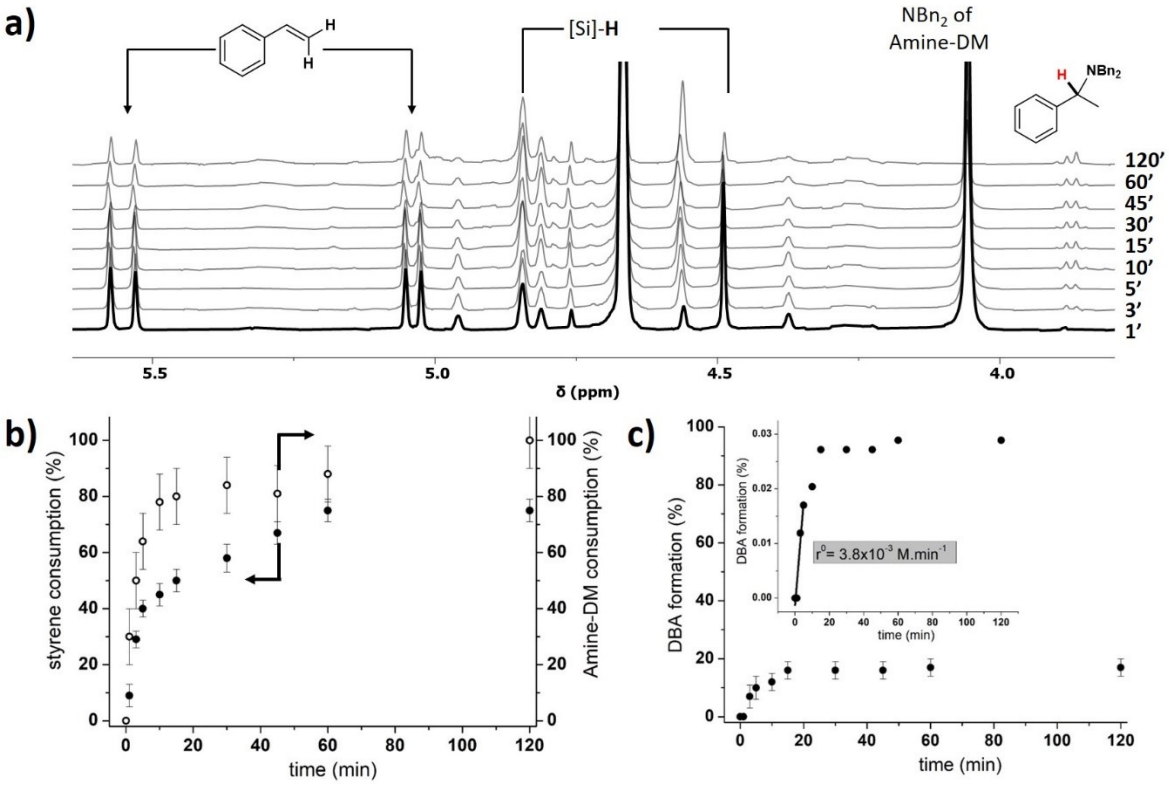

Figure S5 Monitoring of the catalytic reaction with **BTA P^{H}** (initial conditions). (a) ^{1}H NMR spectra between 3.7 and 5.7 ppm for the different reaction times. (b) Plot of the consumption of styrene and **Amine-DM** as a function of reaction time. (c) Plot of the formation of DBA as a function of reaction time. Inset: Determination of the initial rate of DBA formation.

The fact that **Amine-DM** is not fully soluble under these conditions led to a rather large error bar in the determination of the **Amine-DM** consumption (± 10%) from the aliquots.

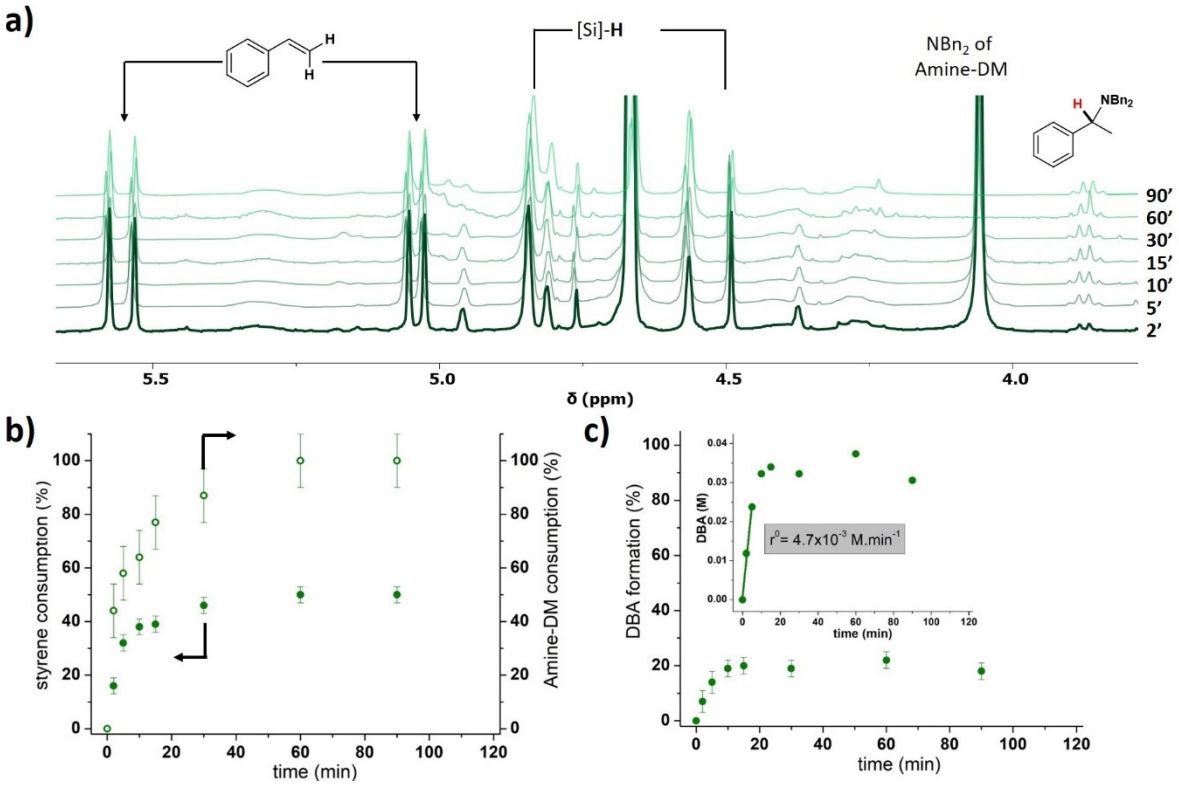

Figure S6 Monitoring of the catalytic reaction with **BTA P^{Me}** (initial conditions). (a) ^{1}H NMR spectra between 3.7 and 5.7 ppm for the different reaction times. (b) Plot of the consumption of styrene and **Amine-DM** as a function of reaction time. (c) Plot of the formation of DBA as a function of reaction time. Inset: Determination of the initial rate of DBA formation.

The fact that **Amine-DM** is not fully soluble under these conditions led to a rather large error bar in the determination of the **Amine-DM** consumption (± 10%) from the aliquots.

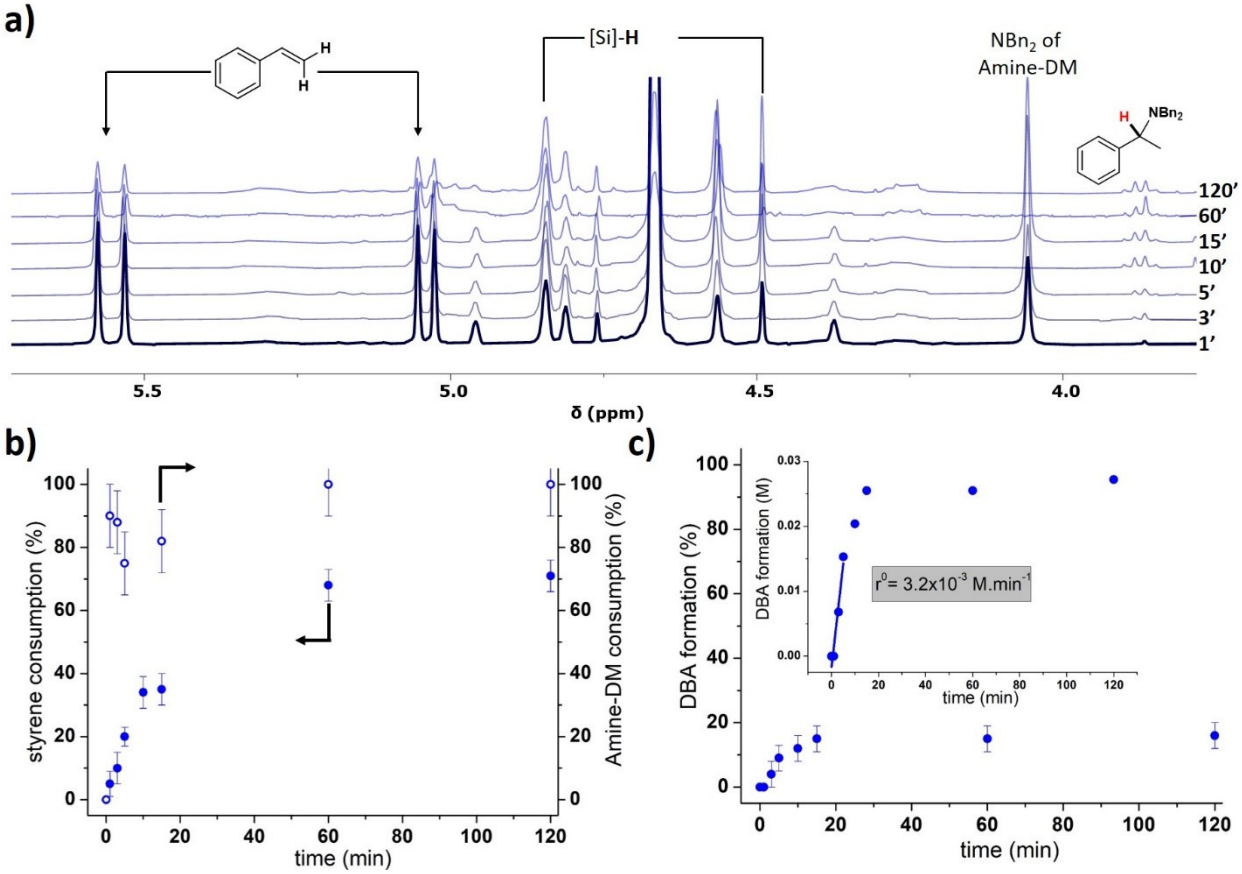

Figure S7 Monitoring of the catalytic reaction with **BTA P$^{p\text{-}F}$** (initial conditions). (a) ^{1}H NMR spectra between 3.7 and 5.7 ppm for the different reaction times. (b) Plot of the consumption of styrene and **Amine-DM** as a function of reaction time. (c) Plot of the formation of DBA as a function of reaction time. Inset: Determination of the initial rate of DBA formation.

The fact that **Amine-DM** is not fully soluble under these conditions led to a rather large error bar in the determination of the **Amine-DM** consumption (± 10%) from the aliquots.

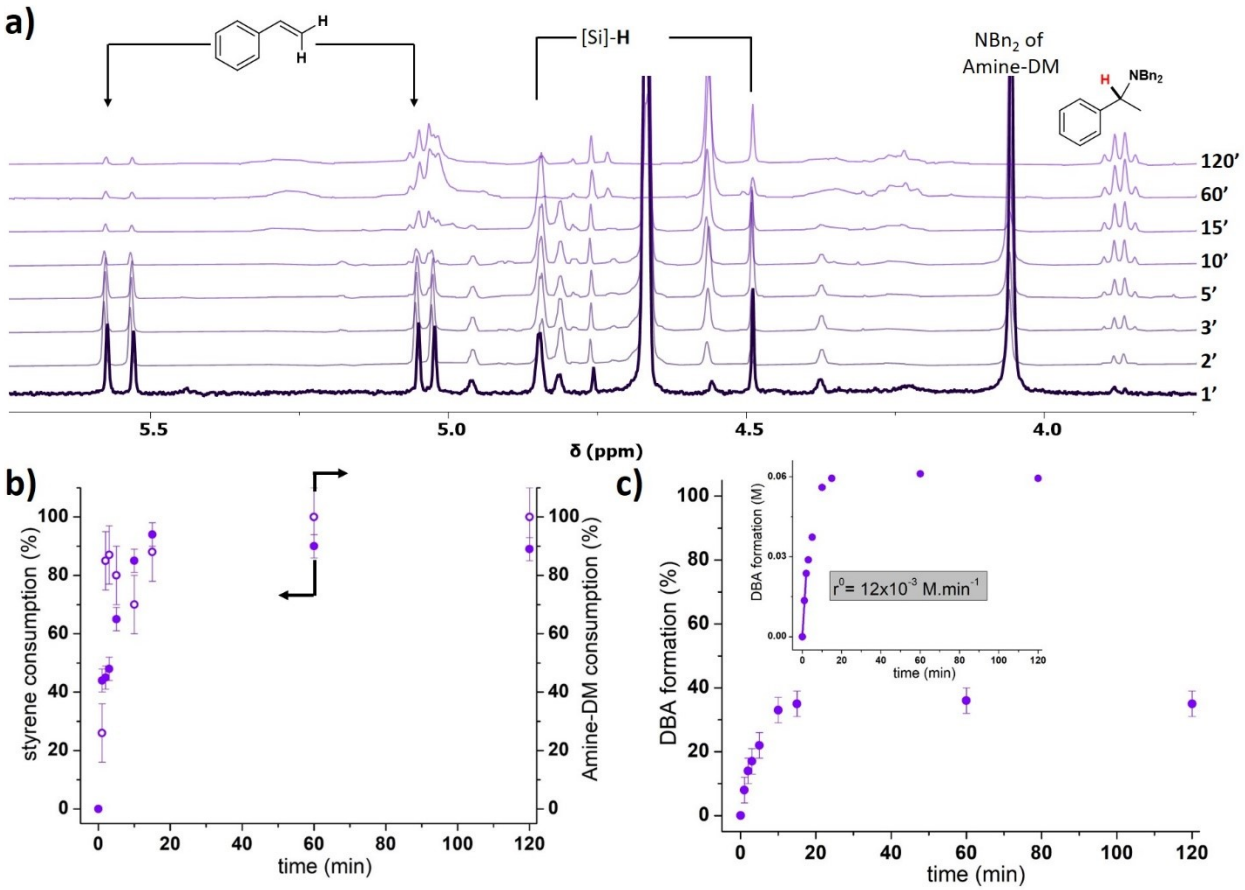

Figure S8 Monitoring of the catalytic reaction with **BTA P$^{p\text{-}CF3}$** (initial conditions). (a) ^{1}H NMR spectra between 3.7 and 5.7 ppm for the different reaction times. (b) Plot of the consumption of styrene and **Amine-DM** as a function of reaction time. (c) Plot of the formation of DBA as a function of reaction time. Inset: Determination of the initial rate of DBA formation.

The fact that **Amine-DM** is not fully soluble under these conditions led to a rather large error bar in the determination of the **Amine-DM** consumption (± 10%) from the aliquots.

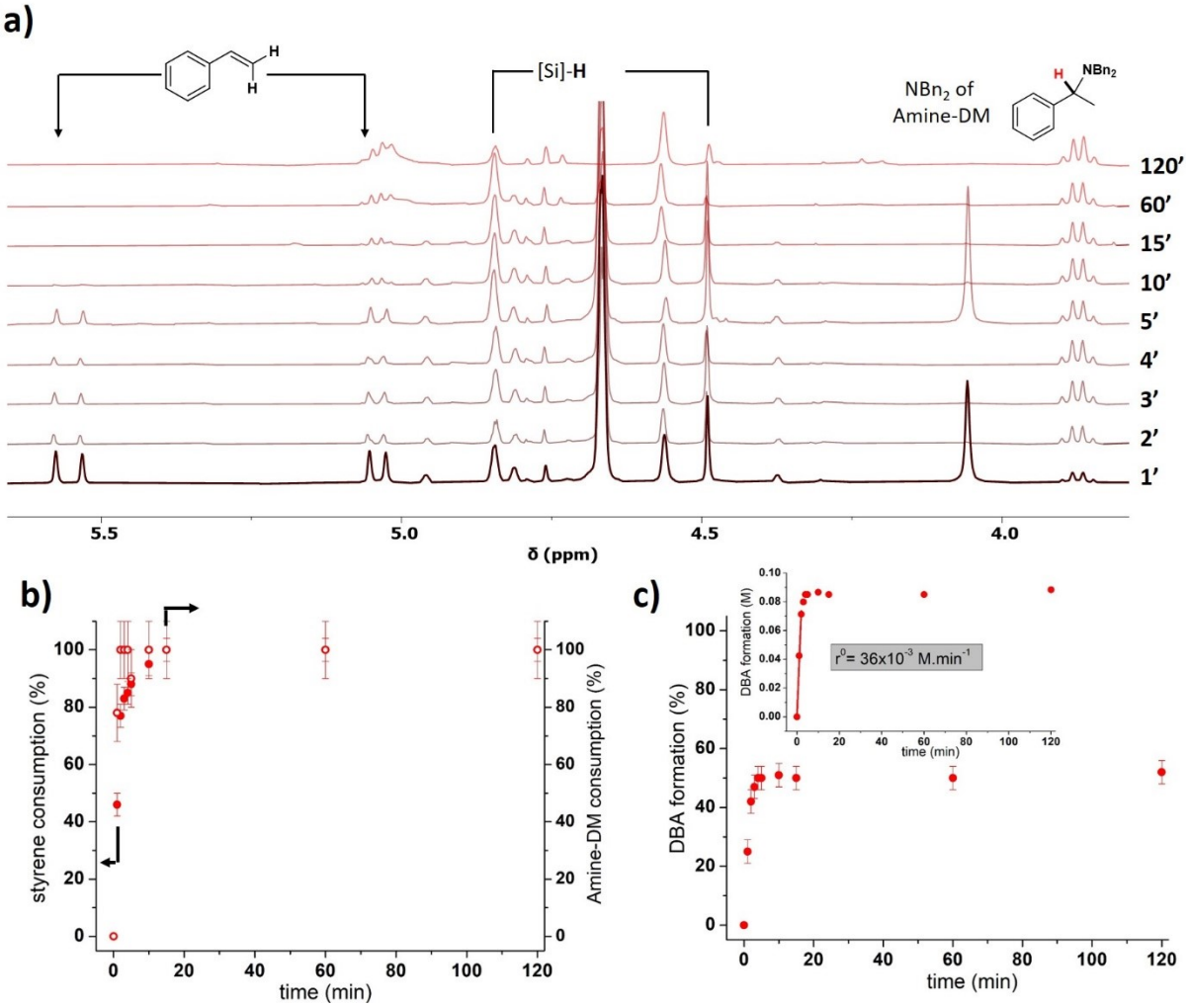

Figure S9 Monitoring of the catalytic reaction with **BTA P^{CF3}** (initial conditions). (a) ^{1}H NMR spectra between 3.7 and 5.7 ppm for the different reaction times. (b) Plot of the consumption of styrene and **Amine-DM** as a function of reaction time. (c) Plot of the formation of DBA as a function of reaction time. Inset: Determination of the initial rate of DBA formation.

The fact that **Amine-DM** is not fully soluble under these conditions led to a rather large error bar in the determination of the **Amine-DM** consumption (± 10%) from the aliquots. This can notably been seen by NMR spectrum recorded at 5' which shows presence of **Amine-DM**, albeit it was not detected for the 2', 3' and 4' spectra.

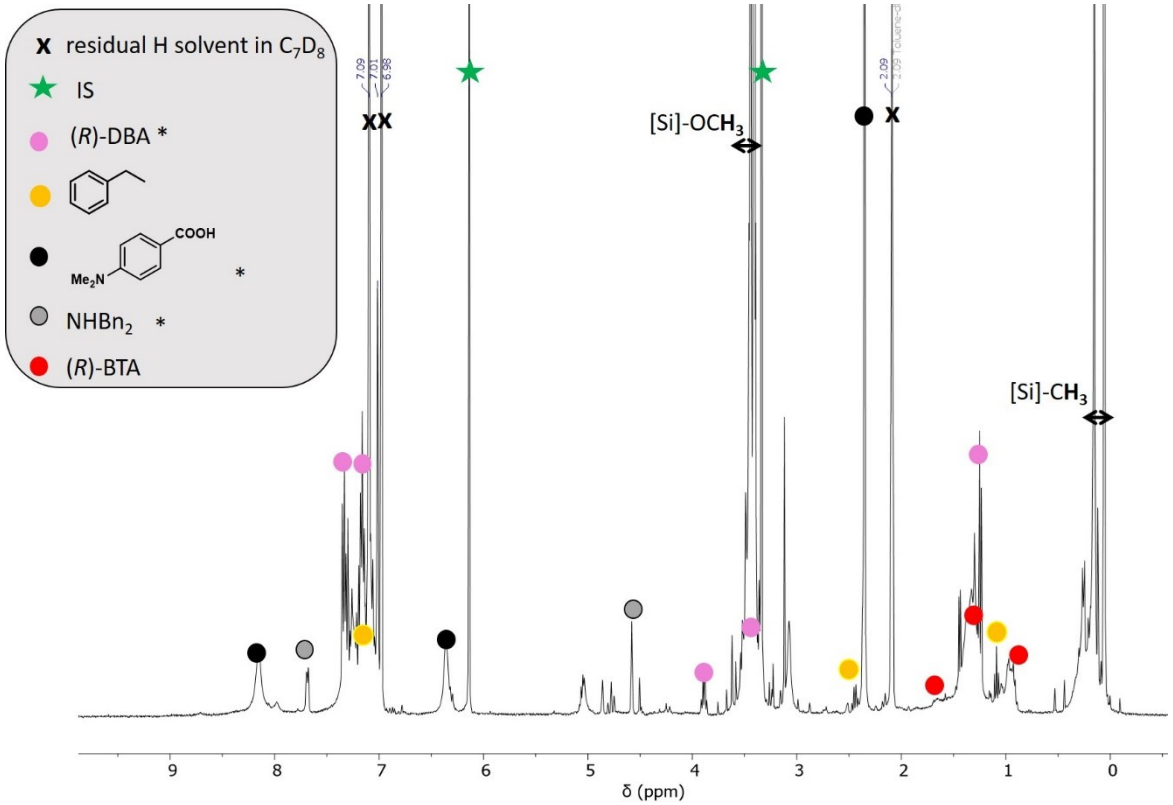

Figure S10 ^{1}H spectrum obtained for catalytic reaction with **BTA P^{CF3}** (initial conditions) after 120' and identification of the main chemical species. *= species also detected by ESI^{+} (see page S-46).

Tables S1 Optimization of the hydroamination reaction of styrene with **BTA P^{CF3}** and **(*R*)-BTA** (f_s^0= 50%).

Optimized parameters:

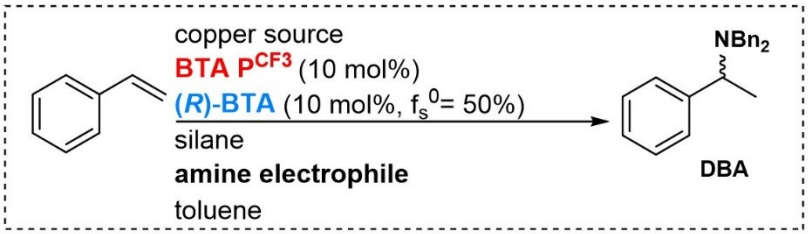

Optimization:
DMMS (*x* mol%)
Temperature
Amine-DM (*x* mol%)
Nature of copper precursor
Nature of silane
Nature of amine electrophile
Concentration in **BTA P^{CF3}**
Cu:**BTA P^{CF3}** ratio

Table S1.1 Amount of DMMS, amount of **Amine-DM**, temperature and repeatability

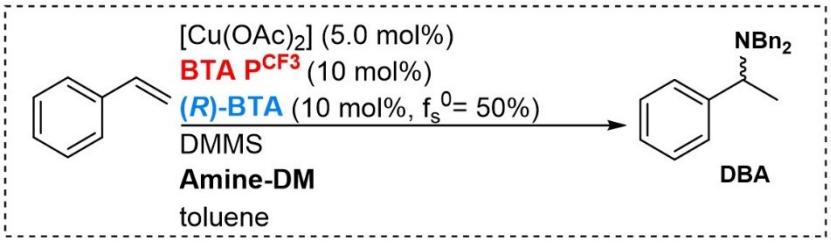

Optimization:
DMMS (*x* mol%)
Temperature
Amine-DM (*x* mol%)

Entry	DMMS (*x* mol%)	**Amine-DM** (*x* mol%)	Temperature (K)	DBA yield (±4 %)[a]	DBA *e.e.* (%)[b]
1	900	120	298	52	68 (*R*)
2	400	120	298	42	69 (*R*)
3	400	120	313	82	68 ±6[c] (*R*)
4	400	120	333	75	63 (*R*)
5	400	180	313	93	69 (*R*)
6	400	180	313	93	69 (*S*)[d]

[a] NMR yield determined by adding 1,3,5-trimethoxybenzene as internal standard.

[b] The optical purity of DBA was determined by HPLC analysis and the configuration of the DBA enantiomers was established according to the literature.[5,6]

[c] The entry was repeated 9 times, yielding the following *e.e.* values: 73%, 65%, 67%, 65%, 63%, 68%, 73%, 70% and 69%. Based on this repeatability assessment, a mean *e.e.* value of 68% can be deduced as well as an error bar of ±6% (equals to ±½ variance). Corresponding NMR yields are 83%, 80%, 80%, 84%, 83%, 80%, 80%, 84% and 80% providing a mean yield of 82% with ±2% error bar (within the experimental error of NMR integration).

[d] **(*S*)-BTA** was used instead of **(*R*)-BTA**.

Table S1.2 Nature of copper precursor and copper: ligand ratio

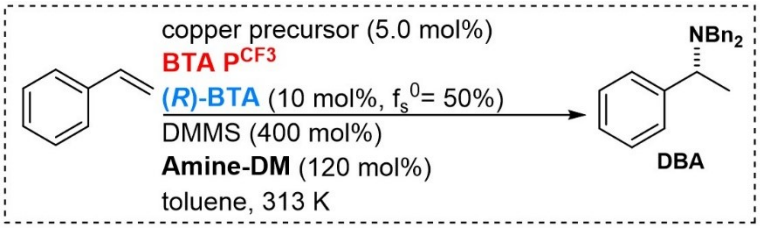

Optimization:
Nature of copper precursor
Cu:**BTA P^{CF3}** ratio

Entry	copper precursor	Cu: **BTA P^{CF3}**	DBA yield (±4 %)[a]	DBA *e.e.* (%)[b]
1	$[Cu(OAc)_2]$	1:2	82	68 ±6 (*R*)
2	$[Cu(OAc)_2]$	1:1	60	66 (*R*)
3	$[Cu(CO_2i\text{-}Pr)_2]$	1:2	80	67 (*R*)
4	[Cu(OAc)]	1:2	84	57 (*R*)
5	CuF_2	1:2	≤ 5	*nd*

[a] NMR yield determined by adding 1,3,5-trimethoxybenzene as internal standard.
[b] The optical purity of DBA was determined by HPLC analysis and the configuration of the DBA enantiomers was established according to the literature.[5,6]
nd= not determined.

Table S1.3 Nature of silane

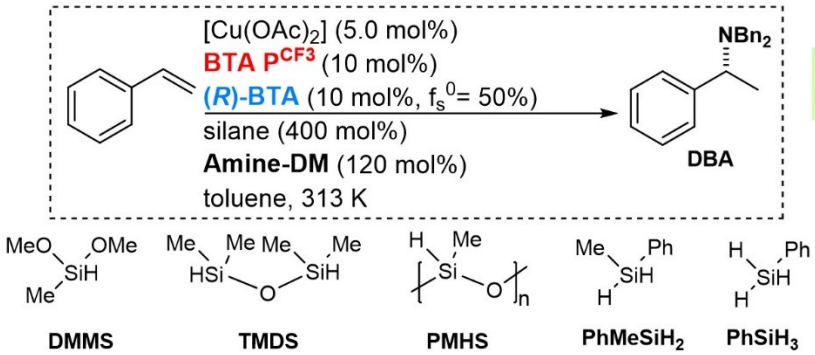

Optimization:
Nature of silane

Entry	silane	DBA yield (±4 %)	DBA *e.e.* (%)
1	DMMS	82	68 ±6 (*R*)
2	TMDS	≤ 5	*nd*
3	PMHS	< 5	*nd*
4	$PhMeSiH_2$	66	74 (*R*)
5	$PhSiH_3$	55	69 (*R*)

Table S1.4 Nature of amine electrophile

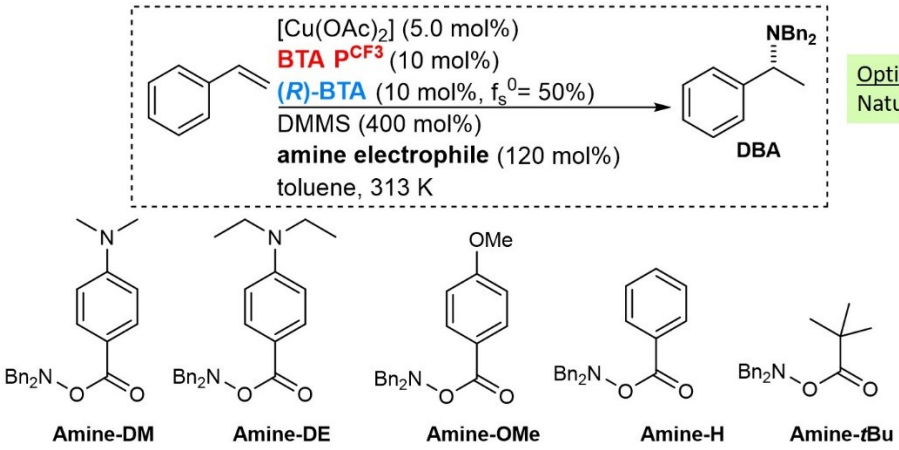

Optimization:
Nature of amine electrophile

Entry	amine electrophile	DBA yield (±4 %)	DBA *e.e.* (%)
1	**Amine-DM**	82	68 ±6 (*R*)
2	**Amine-DE**	84	69 (*R*)
3	**Amine-OMe**	60	72 (*R*)
4	**Amine-H**	66	61 (*R*)
5	**Amine-*t*Bu**	77	73 (*R*)

Table S1.5 Influence of concentration

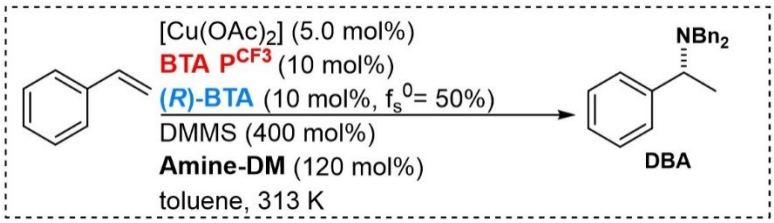

Optimization:
Concentration in **BTA P^{CF3}**

Entry	[**BTA P^{CF3}**] (mM)	DBA yield (±4 %)	DBA *e.e.* (%)
1	17	82	68 ±6 (*R*)
2	10	84	66 (*R*)
3	5	84	66 (*R*)
4	2.5	70	65 (*R*)

Table S2 Optimization of the hydroamination reaction of styrene with **BTA P^{Me}** and **(*R*)-BTA** (f_s^0= 50%).

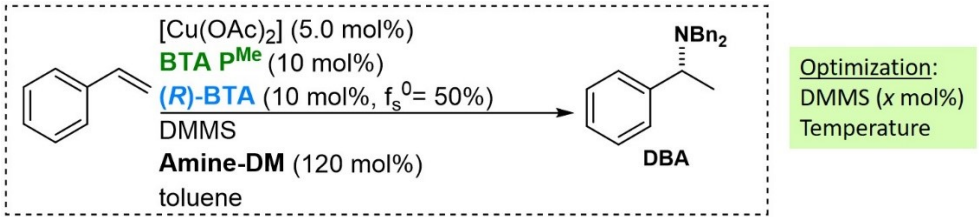

Entry	DMMS (*x* mol%)	Temperature (K)	DBA yield (±4 %)	DBA *e.e.* (%)
1	900	298	22	58
2	400	298	14	55
3	400	313	19	57

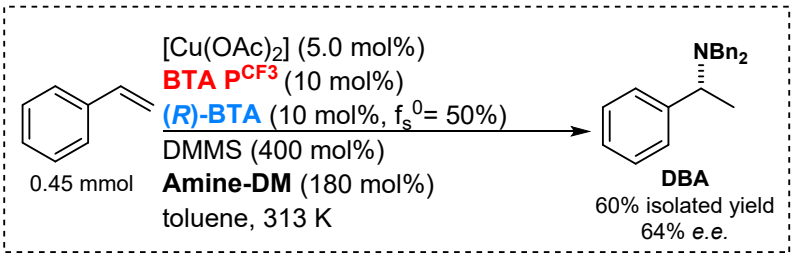

Figure S11 Isolated yield under optimized conditions. For ^{1}H NMR spectrum and HPLC trace of isolated DBA, see page S-40.

Table S3 Composition and catalytic performance for the S&S mixtures composed of **BTA P^{CF3}** and **(*S*)-BTA** with and without **a-BTA**.

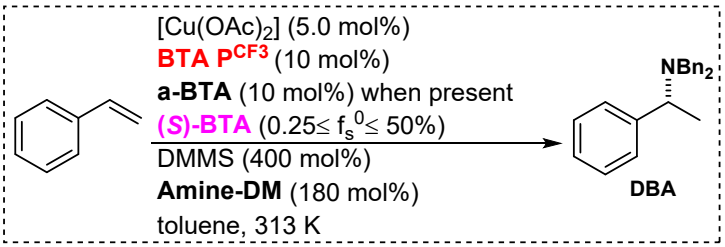

Entry	**a-BTA**	**(*S*)-BTA** (µmol)	**[(*S*)-BTA]** (mM)	**(*S*)-BTA** (mol%)	f_s^0 (%)[a]	yield (%), NMR, isolated	DBA *e.e.* (%)
1	yes	0.23	0.05	0.05	0.26	99, 55	42
2	yes	0.45	0.10	0.10	0.50	96, 66	52
3	yes	0.91	0.19	0.20	1.0	99, 65	62
4	no	0.45	0.10	0.10	1.0	40, 22	10
5	yes	2.31	0.50	0.51	2.5	95, 64	75
6	yes	4.74	1.0	1.05	5.0	97, 64	77
7	yes	10.0	2.1	2.22	10.0	*nd*, 74	81
8	yes	30.0	6.4	6.67	25.0	80, 69	81
9	yes	90.0	18.9	20.0	50.0	90, 69	81
10	no	45.0	9.6	10.0	50.0	87, 69	70

[a] $fs0 = \dfrac{[(S)\text{-BTA}]}{[(S)\text{-BTA}] + [\text{BTA PCF3}] + [\text{a-BTA}]}$

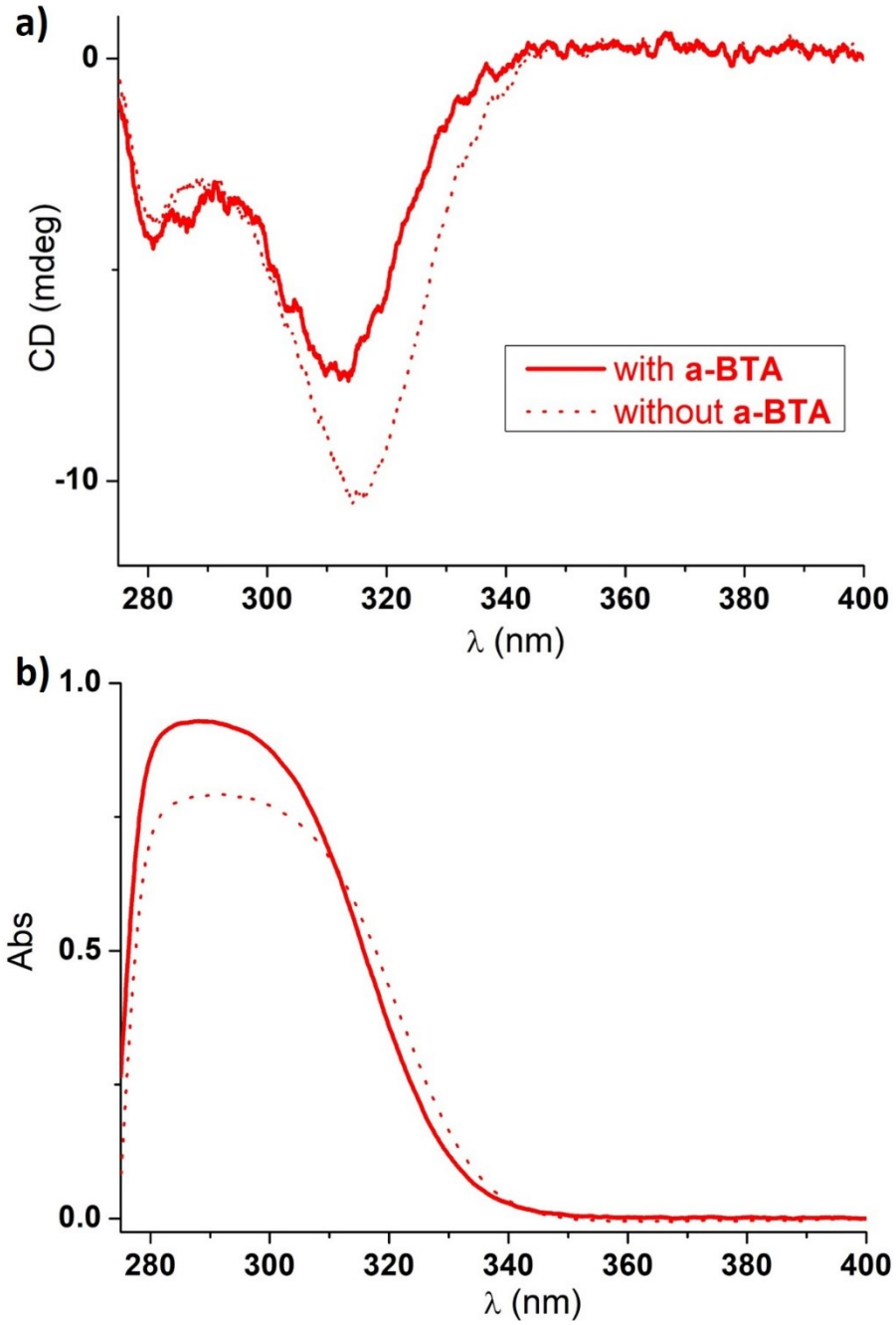

Figure S12 CD (a) and UV-Vis (b) analyses of the S&S mixtures **BTA P^{CF3}** (5.4 mM)/**(*S*)-BTA** (f_s^0= 50%) with and without **a-BTA** (5.4 mM) in toluene-d_8.

The change in the shape and intensity of the ICD signal suggests a different conformation for **BTA P^{CF3}** in the two-component versus three-component BTA system.

Preparation of the solutions

Fourier-Transform Infrared (FT-IR) analyses: A BTA ligand (3.3 mg) and **(*R*)-BTA** (3.3 mg, 3.11 µmol) were mixed in toluene-d_8 (1.0 mL) in order the get the following concentrations in the S&S-type mixtures: **BTA P$^{p\text{-F}}$** (4.58 mM)/**(*R*)-BTA** (3.11 mM, f_s^0=41%) **BTA P$^{p\text{-CF3}}$** (4.02 mM)/**(*R*)-BTA** (3.11 mM, f_s^0=44%), **BTA P^{CF3}** (3.45 mM)/**(*R*)-BTA** (3.11 mM, f_s^0=47%), **BTA P^{H}** (4.82 mM)/**(*R*)-BTA** (3.11 mM, f_s^0=39%), and **BTA P^{Me}** (4.45 mM)/**(*R*)-BTA** (3.11 mM, f_s^0=41%). Samples were briefly heated up to solvent boiling point (≈ 383 K) and analyzed at 293 K.

Circular Dichroism analyses: Mixtures of BTA ligands with **(*S*)-BTA:** A BTA ligand (3.3 mg) and **(*S*)-BTA** (3.3 mg, 3.11 µmol) were mixed in toluene-d_8 (1.0 mL) in order the get the following concentrations in the S&S-type mixtures: **BTA P$^{p\text{-F}}$** (4.57 mM)/**(*S*)-BTA** (3.11 mM, f_s^0=41%), **BTA P$^{p\text{-CF3}}$** (4.02 mM)/**(*S*)-BTA** (3.11 mM, f_s^0=44%), **BTA P^{CF3}** (3.45 mM)/**(*S*)-BTA** (3.11 mM, f_s^0=47%), **BTA P^{H}** (4.81 mM)/**(*S*)-BTA** (3.11 mM, f_s^0=39%), and **BTA P^{Me}** (4.46 mM)/**(*S*)-BTA** (3.11 mM, f_s^0=41%). S&S mixtures of **BTA P^{CF3}** and **(*S*)-BTA** (f_s^0= 50%) with **a-BTA**: **BTA P^{CF3}** (3.64 mg, 3.78 µmol), **a-BTA** (4.12 g, 3.78 µmol), and **(*S*)-BTA** (7.97 mg, 7.56 µmol) were mixed in toluene-d_8 (0.70 mL) in order the get the following concentrations of **BTA P^{CF3}** (5.4 mM), of **a-BTA** (5.4 mM) and of **(*S*)-BTA** (10.8 mM) in the S&S-type mixtures. The sample was briefly heated up to solvent boiling point (≈ 383 K) and analyzed at 293 K. S&S-type mixtures of **BTA P^{CF3}** and **(*S*)-BTA** (f_s^0= 50%) without **a-BTA**: **BTA P^{CF3}** (3.64 mg, 3.78 µmol), and **(*S*)-BTA** (4.00 mg, 3.78 µmol) were mixed in toluene-d_8 (0.70 mL) in order the get the following concentrations of **BTA P^{CF3}** (5.4 mM) and of **(*S*)-BTA** (5.4 mM) in the S&S mixtures. The sample was briefly heated up to solvent boiling point (≈ 383 K) and analyzed at 293 K.

Small Angle Neutron Scattering analyses: A BTA ligand (4.0 mg) and **(*R*)-BTA** (3.9 mg, 3.70 µmol) were mixed in toluene-d_8 (1.2 mL) in order the get the following concentrations in the S&S-type mixtures: **BTA P^{CF3}** (3.33 g.L^{-1}, 3.45 mM)/**(*R*)-BTA** (3.11 mM, f_s^0=47%) and **BTA P^{Me}** (3.33 g.L^{-1}, 4.46 mM)/**(*R*)-BTA** (3.11 mM, f_s^0=41%). The S&S mixture between **BTA P^{H}** (4.0 g.L^{-1}, 5.78 mM) and **(*R*)-BTA** (3.72 mM, f_s^0=39%) have been prepared and analysed previously.[7] All mixtures were briefly heated up to solvent boiling point (≈ 383 K) and analyzed at 293 K.

Catalytic experiments: Screening of the different BTA ligands [17 mM] with the initial conditions: pre-catalytic mixtures composed of the BTA ligand and [$Cu(OAc)_2$] was prepared as follows: oven-dried test tubes were loaded with BTA ligand (15.0 µmol, 10.0 mol%), [$Cu(OAc)_2$] (1.36 mg, 7.5 µmol, 5.0 mol%) and dry THF (500 µL). The solvent was removed under vacuum and the tubes were kept under vacuum (10^{-3} mbar) for 1 hour. **(*R*)-BTA** (15.8 mg, 15.0 µmol, 10 mol%), styrene (17 µL, 0.15 mmol, 100 mol%), **Amine-DM** (64.9 mg, 0.18 mmol, 120 mol%), and 1,3,5-trimethoxybenzene (internal standard, 25.2 mg, 0.15 mmol, 100 mol%) were added to the tubes. Toluene-d_8 (570 µL) was added and the mixture was stirred for 15 minutes at room temperature. The reaction was started by the addition of DMMS (168 µL, 1.35 mmol, 900 mol%). Conversion of

substrate and product yield were monitored by ^{1}H NMR by taking aliquots and diluting them after each time interval. NMR yield of the reaction corresponds to the maximal amount of *N*,*N*-dibenzyl-1-phenylethanamine (DBA) formed (no further evolution of the reaction). Work-up: When reaction was completed, 10% aqueous HCl (400 µL) was added and the mixture was stirred for 30 minutes (until the solution became transparent). Then, the mixture was extracted with Et_2O (3x1 mL). The organic phases were combined and evaporated under vacuum. Acetonitrile was added to the crude and the insoluble material was discarded by filtration. The crude material obtained after evaporation was purified by flash column chromatography over silica gel, eluting with pure DCM. The fractions containing *N*,*N*-dibenzyl-1-phenylethanamine (DBA) were evaporated and analyzed by ^{1}H NMR and chiral HPLC. Chiral HPLC analyses: The optical purity of DBA was determined by HPLC analysis: OD-H column, flow rate: 0.6 mL.min^{-1}, 98:2 hexane/iso-propanol, λ=230 nm, retention time for 1st enantiomer (**(*S*)-DBA**) = 6.7 min, retention time for 2nd enantiomer (**(*R*)-DBA**) = 8.1 min. Configuration of the DBA enantiomers was established according to the literature.[5,6] The enantiomer ratio was determined by HPLC analysis in comparison with authentic racemic material, (*rac*)-DBA, synthesized by adapting literature procedures.[5,6]

Optimization reactions with **BTA P^{CF3}** [*x* mM] and **(*R*)-BTA** (f_s^0= 50%): pre-catalytic mixtures composed of **BTA P^{CF3}** and a *copper source* were prepared as follows: oven-dried test tubes were loaded with **BTA P^{CF3}** (14.5 mg, 15.0 µmol, 10.0 mol%), *a copper source* (*x* mol%) and dry THF (500 µL). The solvent was removed under vacuum and the tubes were kept under vacuum (10^{-3} mbar) for 1 hour. Then styrene (17 µL, 0.15 mmol, 100 mol%) was added before flushing the tube with argon for 10 seconds. **(*R*)-BTA** (15.8 mg, 15.0 µmol), *an amine electrophile* (*x* mol%), and 1,3,5-trimethoxybenzene (internal standard, 25.2 mg, 0.15 mmol, 100 mol%) were added as solids. Toluene-d_8 (*x* µL) was added and the mixture was stirred for 15 minutes at room temperature. The reaction mixture was placed at the desired *temperature* and the reaction was started by the addition of a *silane* (*x* mol%). Conversion of substrate and product yield were monitored by ^{1}H NMR by taking aliquots and diluting them after each time interval. Work-up and purification were performed as indicated above.

Optimization reactions with **BTAP^{Me}** [17 mM] and **(*R*)-BTA** (f_s^0= 50%): pre-catalytic mixtures composed of **BTA P^{Me}** and [$Cu(OAc)_2$] was prepared as follows: oven-dried test tubes were loaded with **BTA P^{Me}** (11.2 mg, 15.0 µmol, 10.0 mol%), [$Cu(OAc)_2$] (1.36 mg, 7.5 µmol, 5.0 mol%) and dry THF (500 µL). The solvent was removed under vacuum and the tubes were kept under vacuum (10^{-3} mbar) for 1 hour. Then styrene (17 µL, 0.15 mmol, 100 mol%) was added before flushing the tube with argon for 10 seconds. **(*R*)-BTA** (15.8 mg, 15.0 µmol), **Amine-DM** (64.9 mg, 0.18 mmol, 120 mol%), and 1,3,5-trimethoxybenzene (internal standard, 25.2 mg, 0.15 mmol, 100 mol%) were added as solids. Toluene-d_8 (570 µL) was added and the mixture was stirred for 15 minutes at room temperature. The reaction mixture was placed at the desired *temperature* and the reaction was started by the addition of DMMS (*x* mol%). Conversion of substrate and product yield were monitored by

^{1}H NMR by taking aliquots and diluting them after each time interval. Work-up and purification were performed as indicated above.

Isolated yield under optimized conditions (**BTA P^{CF3}** [18 mM]): an oven-dried test tube was loaded with **BTA P^{CF3}** (43.4 mg, 45.0 μmol, 10.0 mol%), [Cu(OAc)$_2$] (4.1 mg, 22.5 μmol, 5.0 mol%) and dry THF (500 μL). The solvent was removed under vacuum and the tube was kept under vacuum (10^{-3} mbar) for 1 hour. **(*S*)-BTA** (47.5 mg, 45.0 μmol, 10.0 mol%) and toluene (1800 μL) were added to the tube and the mixture was briefly heated to reflux and stirred for 15 minutes at room temperature. Styrene (51 μL, 0.45 mmol, 100 mol%) and **Amine-DM** (292 mg, 0.81 mmol, 180 mol%) were added to the tube and the tube was flushed with argon for 10 seconds. The reaction mixture was heated to 40°C and DMMS was added (223 μL, 1.8 mmol, 400 mol%). After 2 hours, the reaction mixture was cooled down to room temperature and 2 mL of a saturated aqueous solution of Na_2CO_3 was added as well as ethyl acetate (1 mL). The phases were separated and the aqueous layer was extracted with ethyl acetate (2×1 mL). The organic phases were combined and evaporated under vacuum. Acetonitrile was added to the crude and the insoluble material was discarded by filtration. The crude material obtained after evaporation was purified by flash column chromatography over silica gel, eluting with dichloromethane/ethyl acetate yielding (*S*)-DBA as a colorless oil (81 mg, 60% yield, 63% *e.e.*). The analytical data of (*S*)-DBA are in agreement with the literature (see pages S-40).[5,6]

Sergeants-and-soldiers-type experiments with **BTA P^{CF3}** [9.6 mM] and **(*S*)-BTA**: In presence of **a-BTA**: an oven-dried test tube was loaded with **BTA P^{CF3}** (43.4 mg, 45.0 μmol, 10.0 mol%), [Cu(OAc)$_2$] (4.1 mg, 22.5 μmol, 5.0 mol%) and dry THF (500 μL). The solvent was removed under vacuum and the tube was kept under vacuum (10^{-3} mbar) for 1 hour. **(*S*)-BTA** (0.23−90 μmol, 0.05−20.0 mol%), **a-BTA** (49.1 mg, 45.0 μmol, 10.0 mol%), and toluene (4000 μL) were added to the tube and the mixture was briefly heated to reflux and stirred for 15 minutes at room temperature. Styrene (51 μL, 0.45 mmol, 100 mol%), and **Amine-DM** (292 mg, 0.81 mmol, 180 mol%) were added to the tube and the tube was flushed with argon for 10 seconds. The reaction mixture was heated to 40°C and DMMS was added (223 μL, 1.8 mmol, 400 mol%). After 2 hours, the reaction mixture was cooled down to room temperature and 2 mL of a saturated aqueous solution of Na_2CO_3 was added as well as ethyl acetate (1 mL). The phases were separated and the aqueous layer was extracted with ethyl acetate (2×1 mL). 1,3,5-trimethoxybenzene (75.7 mg, 0.45 mmol, 100 mol%) was added to the combined organic phases and the NMR yield was established after evaporation of the solvent. Acetonitrile was added to the crude and the insoluble material was discarded by filtration. The crude material was purified by flash column chromatography over silica gel, eluting with dichloromethane/ethyl acetate yielding (*S*)-DBA as a colorless oil (see isolated yields in Table S.3). The optical purity of DBA in each sergeants-and-soldiers mixture was determined by chiral HPLC (pages S-41 to S-45). In absence of **a-BTA**: an oven-dried test tube was loaded with **BTA P^{CF3}** (43.4 mg, 45.0 μmol, 10.0 mol%), [Cu(OAc)$_2$] (4.1 mg, 22.5 μmol, 5.0 mol%) and dry THF

(500 μL). The solvent was removed under vacuum and the tube was kept under vacuum (10^{-3} mbar) for 1 hour. **(*S*)-BTA** (0.45−22.5 μmol, 0.1 and 5.0 mol% respectively) and toluene (4000 μL) were added to the tube and the mixture was briefly heated to reflux and stirred for 15 minutes at room temperature. Styrene (51 μL, 0.45 mmol, 100 mol%), and **Amine-DM** (292 mg, 0.81 mmol, 180 mol%) were added to the tube and the tube was flushed with argon for 10 seconds. The reaction mixture was heated to 40°C and DMMS was added (223 μL, 1.8 mmol, 400 mol%). After 2 hours, the reaction mixture was cooled down to room temperature and 2 mL of a saturated aqueous solution of Na_2CO_3 was added as well as ethyl acetate (1 mL). The phases were separated and the aqueous layer was extracted with ethyl acetate (2×1 mL). 1,3,5-trimethoxybenzene (75.7 mg, 0.45 mmol, 100 mol%) was added to the combined organic phases and the NMR yield was established after evaporation of the solvent. Acetonitrile was added to the crude and the insoluble material was discarded by filtration. The crude material was purified by flash column chromatography over silica gel, eluting with dichloromethane/ethyl acetate yielding (*S*)-DBA as a colorless oil (see isolated yields in Table S.3). The optical purity of DBA in each sergeants-and-soldiers mixture was determined by chiral HPLC (pages S-41 to S-45).

Material and methods

Materials: The synthetic procedures for the preparation of **BTA P$^{p\text{-F}}$**, **BTA P$^{p\text{-CF3}}$** and **BTA P^{CF3}** are described below. The syntheses of **BTA P^{H}**,[4] and **BTA P^{Me}**,[8] and **a-BTA**[8] were reported previously. Amine electrophiles (NBn_2-OR), *O*-benzoyl-*N*,*N*-dibenzylhydroxylamine (**Amine-H**), *N*,*N*-dibenzyl-*O*-(4-trimethoxybenzoyl)hydroxylamine (**Amine-OMe**), *N*,*N*-dibenzyl-*O*-pivaloylhydroxylamine (**Amine-*t*Bu**), 4-(((dibenzylamino)oxy)carbonyl)-*N*,*N*-diethylaniline (**Amine-DE**) and 4-(((dibenzylamino)oxy)carbonyl)-*N*,*N*-dimethylaniline (**Amine-DM**) were synthesized by reacting *N*,*N*-dibenzylhydroxylamine with the corresponding carboxylic acid derivatives in presence of *N*,*N*'-carbonyldiimidazole (CDI) as described in the literature.[6,9] **(*R*)-BTA** and **(*S*)-BTA** have been prepared according to a published protocole (*ee*> 99%, *de*> 90%).[7,10] Styrene (Sigma-Aldrich, 99%) was distilled under vacuum prior to use. Bis(4-fluorophenyl)chlorophosphine (Alfa Aesar, 98%), bis(4-(trifluoromethyl)phenyl)chlorophosphine (Alfa Aesar, 97%), bis(3,5- (trifluoromethyl)phenyl)chlorophosphine (Alfa Aesar, 98%), 4-[bis(trimethylsilyl)amino]phenylmagnesium bromide (provided as 1.0 M solution in THF, Sigma-Aldrich), 4-bromo-*N*,*N*-bis(trimethylsilyl)aniline (Alfa Aesar, 97%), DMAP (Sigma-Aldrich, 99%), EDC·HCl (abcr, 98%), *N*,*N*'-carbonyldiimidazole (CDI, Sigma-Aldrich, 97%), dimethoxy(methyl)silane (DMMS, Fluorochem, 97%), 1,1,3,3-tetramethyldisiloxane (TMDS, Sigma-Aldrich, 97%), polymethylhydrosiloxane (PMHS, Sigma-Aldrich, average M_n 1.700-3.200), methylphenylsilane ($PhMeSiH_2$, Sigma-Aldrich, 98%), phenylsilane ($PhSiH_3$, Sigma-Aldrich, 97%), [$Cu(OAc)_2$] (Sigma-Aldrich, 99.99%), [CuOAc] (Sigma-Aldrich, 97%), [CuF_2] (Alfa Aesar, 99.5%), and [$Cu(CO_2i\text{-}Pr)_2$] (copper *iso*-butyrate, Strem, 99%) were used as received. Dried THF, Et_2O and toluene were obtained from a Solvent Purification System (SPS). Toluene-d_8 for spectroscopic analyses was obtained from Eurisotop (99.5% D) and used as received.

Methods: **NMR analyses**: NMR spectra were recorded on a Bruker Avance 400 spectrometer and calibrated to the residual solvent peak: DMSO-d_6 (^{1}H: 2.50 ppm, ^{13}C: 39.52 ppm), toluene-d_8 (^{1}H: 2.08, 6.97, 7.01, 7.09 ppm, ^{13}C: 137.48, 128.87, 127.96, 125.13, 20.43 ppm) and C_6D_6 (^{1}H: 7.16 ppm, ^{13}C: 128.06 ppm). Peaks are reported with their corresponding multiplicity (s: singlet; d: doublet; dd: doublet of doublets; dq: doublet of quartets; q: quartet, m: multiplet) coupling constants and integration.

HRMS analyses: Exact mass measurements (HRMS) were obtained on TQ R30-10 HRMS spectrometer by ESI^+ ionization and are reported in *m/z* for the major signal.

FT-IR analyses: Fourier-Transform Infrared (FT-IR) measurements were performed on a Nicolet iS10 spectrometer. Spectrum for the solids was recorded by evaporating a small amount of its solution in methanol over a KBr plate and the main peaks were reported as m: medium, s: strong, w: weak, br: broad. Spectra of solutions of BTA ligands, **(*R*)-BTA** and of their S&S-type mixtures in toluene-d_8 were recorded at 293 K in CaF_2 cells with 0.05 cm path length and were corrected for air, toluene and cell absorption.

CD analyses: Circular dichroism (CD) measurements were performed equipped with a Peltier thermostated cell holder and Xe laser. CD spectra were recorded at 293 K with the following parameters: 50 nm.min^{-1} sweep rate, 0.05 nm data pitch, 2.0 nm bandwidth, and between 400 and 275 nm with solutions placed into cylindrical spectrosil quartz cells of 0.10 mm pathlength (Starna® 31/Q/0.1) for analyses of BTA ligands and **(*S*)-BTA** mixtures (Figure S4) or into dismountable quartz cells of 0.10 mm pathlength for S&S-type mixtures of **BTA P^{CF3}**, **(*S*)-BTA** and **a-BTA** (Figure S12). All solutions were pre-heated before measurements. Toluene-d_8 and cell contributions at the same temperature were subtracted from the obtained signals. For all samples, LD contribution was negligible (ΔLD < 0.005 dOD) and the shape of the CD signal was independent of the orientation of the quartz cells.

UV-Vis analyses: UV-Vis absorption spectra were extracted from CD analyses on each of the above samples and obtained after correction of the absorption of air, solvent, and cell contribution at the same temperature.

SANS analyses: Small-angle neutron scattering (SANS) measurements were made at the LLB (Saclay, France) on the PA20 instrument, at two (or three) distance-wavelength combinations to cover the 3.65×10^{-3} (or 2.45×10^{-3} for the mixture between **BTA P^{H}** and **(*R*)-BTA**) to 0.3 Å q^{-1} range, where the scattering vector q is defined as usual, assuming elastic scattering, as $q = (4\pi/\lambda)\sin(\theta/2)$, where θ is the angle between incident and scattered beam. Data were corrected for the empty cell signal and the solute and solvent incoherent background. A light water standard was used to normalize the scattered intensities to cm^{-1} units. The data for the mixtures was modelled by the combination of cylinders of infinite length and of spheres. The cylinders are assumed to be composed of BTA ligand molecules and a fraction of **(*R*)-BTA**. The spheres are assumed to consist in the remaining **(*R*)-BTA** molecules. The only adjustable parameters were the proportion of sergeants that co-assemble with the BTA ligand into cylinders. The radius of cylinders and spheres were fixed to 12±1 Å and 11±1 Å, respectively, because these values are consistent with the radius obtained by fitting the SANS curves in C_7D_8 of the individual components of the previously investigated S&S-type mixtures.[7,11]

The scattering length densities (SLD) for the spheres were calculated from the atomic bound coherent scattering lengths (see Table S4). The SLD for the cylinders were calculated by averaging the molecular SLD according to the composition of the cylinders.

Table S4: values of the scattering length densities.

	toluene-d_8	**BTA P^{H}**	**BTA P^{Me}**	**BTA P^{CF3}**	**(*R*)-BTA**
ρ (10^{-6} Å^{-2})	5.66	1.17	1.06	1.52	0.479

Determination of f_s^s values by FT-IR analyses: FT-IR measurements were performed on a Nicolet iS10 spectrometer. Spectra of solutions in toluene were measured in 0.05 cm pathlength CaF_2 cells

at 293 K and were corrected for air, solvent and cell absorption. The fraction of sergeants in the different S&S-type mixtures was determined following our previously described procedure.[7] The influence of stack ends was neglected since free N−H are hardly detected in the FT-IR spectra of the mixtures (Figure S2). The concentration of dimers is extracted by fitting the ester carbonyl region of the experimental FT-IR spectrum of the S&S-type mixtures (1700-1800 cm^{-1}) with the individual spectra of **(*R*)-BTA** (representative of sergeants in dimers, bonded ester CO, ν≈ 1725 cm^{-1}) and of **BTA Met**[2-3] (reference for sergeants in stacks, free ester CO, ν≈ 1745 cm^{-1}). It yields the following concentrations of **(*R*)-BTA** in stacks: 2.0±0.2 mM (for **BTA P^{H}**), 1.7±0.2 mM (for **BTA P^{Me}**), 2.2±0.2 mM (for **BTA $P^{p\text{-}F}$**), 2.1±0.2 mM (for **BTA $P^{p\text{-}CF3}$**), and 2.2±0.2 mM (for **BTA P^{CF3}**). The addition of the FT-IR spectra of the remaining **(*R*)-BTA** dimers, of the BTA ligand (3.33 $g.L^{-1}$) and of **BTA Met** (at the concentration of the sergeant in stacks) yields the simulated spectra shown in Figure S2. Since the FT-IR spectrum of **BTA P^{CF3}** alone cannot be recorded as it is poorly soluble in toluene, the FT-IR spectrum of **BTA P^{H}** was used instead for the simulation.

Synthesis of BTA ligands

Synthesis of BTA P$^{p\text{-}F}$

- Step 1: synthesis of 4-(bis(4-fluorophenyl)phosphino)aniline

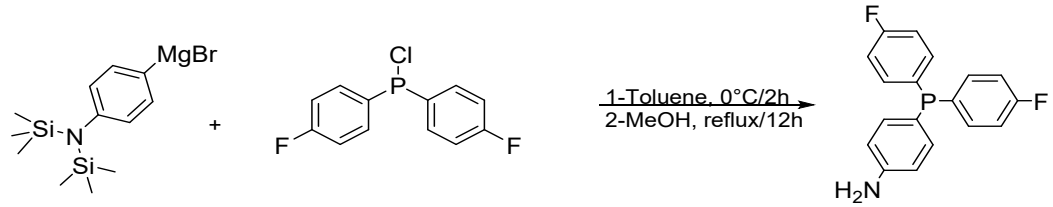

Bis(4-fluorophenyl)chlorophosphine (3.0 g, 11.7 mmol, 1.2 equiv.) in dry toluene was added dropwise to a 1 M solution of 4-[bis(trimethylsilyl)amino]phenylmagnesium bromide (9.7 mL, 9.7 mmol, 1.0 equiv.) in toluene at 0 °C. The reaction mixture was stirred for 2 hours at 0°C. The reaction was monitored by $^{31}P\{^{1}H\}$ NMR. The volatiles were removed under vacuum and the solid residue was extracted with dry Et_2O via a cannula to another three-neck round-bottom flask equipped with a special fritted funnel designed to perform filtrations under argon. Et_2O was removed under vacuum, the crude product was then dissolved in MeOH (10 mL) and the solution was stirred at reflux temperature for one day under argon. The solution was evaporated under vacuum, and the crude product was purified by flash column chromatography over silica gel, eluting with DCM/methanol 99:1–95:5 gradient, yielding 4-(bis(4-fluorophenyl)phosphino)aniline (400 mg, 13% yield) as a colorless solid. ^{1}H NMR (400 MHz, toluene-d_8): δ (ppm) 7.20 – 7.11 (m, 6H), 6.75 (t, *J*= 8.5 Hz, 4H), 6.22 (d, 2H), 2.86 (br s, 2H) ppm. $^{31}P\{^{1}H\}$ NMR (122 MHz, toluene-d_8) δ (ppm) = -8.7. $^{19}F\{^{1}H\}$ NMR (122 MHz, DMSO-d_6) δ (ppm) -113.0.

- Step 2: synthesis of **BTA P$^{p\text{-}F}$**

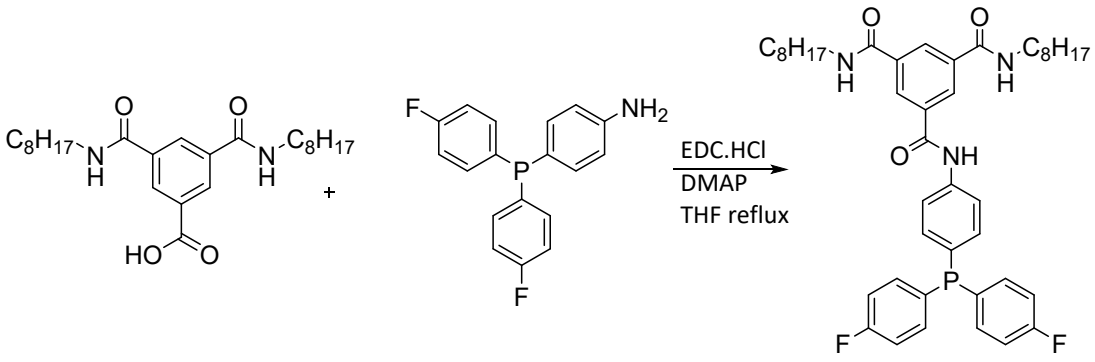

3,5-bisoctylaminocarbonyl-benzoic acid[12] (430 mg, 1.0 mmol, 1.0 equiv.) was suspended in THF (30 mL) under argon and DMAP (175 mg, 1.43 mmol, 1.4 equiv.), EDC·HCl (275 mg, 1.43 mmol, 1.4 equiv.) and 4-(bis(4-fluorophenyl)phosphino)aniline (400 mg, 1.28 mmol, 1.3 equiv.) were added to the flask. The reaction mixture was stirred at reflux temperature for two days under argon.

Then the reaction mixture was cooled to room temperature, and the solvent was evaporated under vacuum. DCM was added to the residue, and the organic layer was washed three times with water. Organic layers were combined, dried over magnesium sulfate and evaporated under vacuum. The crude product was purified by flash column chromatography over silica gel, eluting with DCM/ethyl acetate 95:5–88:12 gradient, yielding **BTA P$^{p\text{-}F}$** (338 mg, 47% yield) as a colorless solid. ^{1}H NMR (400 MHz, DMSO-d_6) δ (ppm) 10.63 (s, 1H, ArNH), 8.69 (t, *J*= 5.6 Hz, 2H, CH_2NH), 8.47 (s, 2H, BTA ring), 8.44 (s, 1H, BTA ring), 7.85 (d, *J*= 8.2 Hz, 2H, $CH_{arom.}$ linker), 7.38 – 7.20 (m, 10H, 2× $CH_{arom.}$ linker + PAr_2), 3.30 – 3.26 (m, 4H, CH_2NH), 1.60 – 1.48 (m, 4H, CH_2CH_2NH), 1.34 – 1.16 (m, 20H, CH_2), 0.85 (t, *J*= 6.4 Hz, 6H, CH_3). ^{31}P{^{1}H} NMR (162 MHz, DMSO-d_6) δ (ppm) -10.2. ^{19}F{^{1}H} NMR (377 MHz, DMSO-d_6) δ (ppm) -112.3. ^{13}C{^{1}H} NMR (101 MHz, DMSO-d_6) δ (ppm) 165.19 (C=O), 165.07 (C=O), 162.55 (d, *J*= 247.0 Hz, $C_{arom.}$-F),[13] 140.05 ($C_{arom.}$), 135.35 (dd, *J*= 20.9, 8.1 Hz, $CH_{arom.}$), 135.20 ($C_{arom.}$), 135.18 ($C_{arom.}$), 133.80 (d, *J*= 20.7 Hz, $CH_{arom.}$), 132.85 (dd, *J*= 11.6, 3.2 Hz, $C_{arom.}$-P), 130.80 (d, *J*= 9.7 Hz, $C_{arom.}$-P), 128.97 ($CH_{arom.}$), 128.80 ($CH_{arom.}$), 120.47 (d, *J*= 7.4 Hz, $CH_{arom.}$), 115.95 (dd, *J*= 21.0, 7.5 Hz, $CH_{arom.}$), 39.39 (CH_2), 31.25 (CH_2), 29.01 (CH_2), 28.75 (CH_2), 28.66 (CH_2), 26.50 (CH_2), 22.08 (CH_2), 13.91 (CH_3). HRMS (ESI, m/z): Calculated for $C_{43}H_{52}F_2N_3O_3PH$, $[M+H]^+$: 728.3787, found: 728.3791. FT-IR (KBr plates, cm^{-1}): 646 (m), 690 (m), 710 (m), 825 (s), 1012 (w), 1087 (m), 1117 (m), 1157 (s), 1181 (m), 1222 (m), 1251 (m), 1287 (m), 1311 (m), 1392 (m), 1494 (s), 1520 (s), 1585 (s), 1633 (s), 2853 (m), 2924 (m), 2953 (w), 3086 (w), 3253 (br).

Synthesis of BTA P$^{p\text{-}CF3}$

- Step 1: synthesis of 4-(bis(4-(trifluoromethyl)phenyl)phosphino)aniline

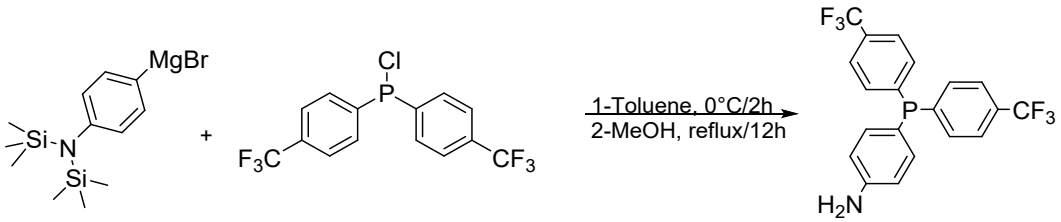

Bis(4-(trifluoromethyl)phenyl)chlorophosphine (1.0 g, 2.8 mmol, 1.2 equiv.) in dry toluene was added dropwise to a 1 M solution of 4-[bis(trimethylsilyl)amino]phenylmagnesium bromide (2.4 mL, 2.34 mmol, 1.0 equiv.) at 0 °C. The reaction mixture was stirred for 2 hours at 0°C. The reaction was monitored by ^{31}P{^{1}H} NMR. The volatiles were removed under vacuum and the solid residue was extracted with dry Et_2O via a cannula to another three-neck round-bottom flask equipped with a special fritted funnel designed to perform filtrations under argon. Et_2O was removed under vacuum, the crude product was then dissolved in MeOH (10 mL) and the solution was stirred at reflux temperature for one day under argon. The solution was evaporated under vacuum, and the crude product was purified by flash column chromatography over silica gel, eluting with DCM/methanol 99:1–95:5 gradient, yielding 4-(bis(4-

(trifluoromethyl)phenyl)phosphino)aniline (500 mg, 52% yield) as a colorless solid. ^{1}H NMR (400 MHz, toluene-d_8) δ (ppm) 7.26 – 7.15 (m, 4H), 7.14 – 7.04 (m, 6H), 6.16 (d, *J*= 8.0 Hz, 2H), 2.82 (br s, 2H, NH_2). ^{31}P{^{1}H} NMR (122 MHz, C_6D_6) δ (ppm) -6.5.

- Step 2: synthesis of **BTA P$^{p\text{-CF3}}$**

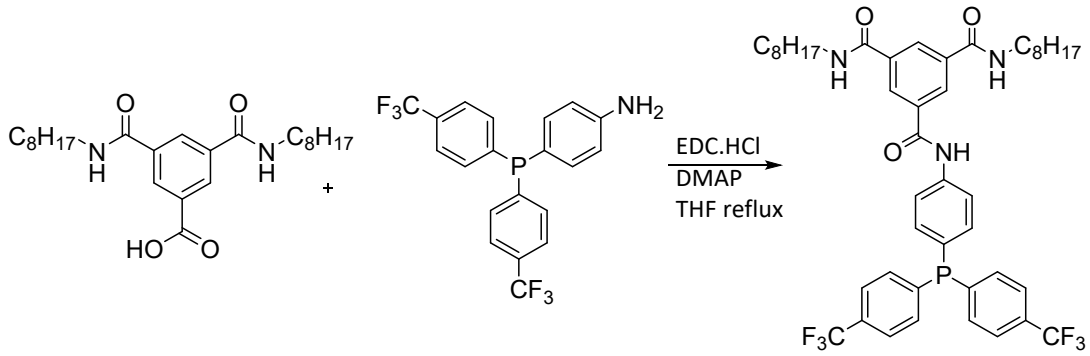

3,5-bisoctylaminocarbonyl-benzoic acid[12] (417 mg, 0.97 mmol, 1.0 equiv.) was suspended in THF (30 mL) under argon and DMAP (166 mg, 1.36 mmol, 1.5 equiv.), EDC·HCl (260 mg, 1.36 mmol, 1.5 equiv.) and 4-(bis(4-(trifluoromethyl)phenyl)phosphino)aniline (500 mg, 1.21 mmol, 1.1 equiv.) were added to the flask. The reaction mixture was stirred at reflux temperature for two days under argon. Then the reaction mixture was cooled to room temperature, and the solvent was evaporated under vacuum. DCM was added to the residue, and the organic layer was washed three times with water. Organic layers were combined, dried over magnesium sulfate and evaporated under vacuum. The crude product was purified by flash column chromatography over silica gel, eluting with DCM/ethyl acetate 95:5–88:12 gradient, yielding **BTA P$^{p\text{-CF3}}$** (543 mg, 68% yield) as a colorless solid. ^{1}H NMR (400 MHz, DMSO-d_6): δ (ppm) 10.69 (s, 1H, ArNH), 8.69 (t, *J*= 5.3 Hz, 2H, $CH_2N\mathit{H}$), 8.48 (s, 2H, BTA ring), 8.45 (s, 1H, BTA ring), 7.92 (d, *J*= 8.2 Hz, 2H, $CH_{arom.}$ linker), 7.79 (d, *J*= 7.9 Hz, 4H, PAr_2), 7.48 (t, *J*= 7.4 Hz, 4H, PAr_2), 7.38 (t, *J*= 8.0 Hz, 2H, $CH_{arom.}$ linker), 3.40 – 3.16 (m, 4H, $C\mathit{H}_2NH$), 1.61 – 1.47 (m, 4H, $C\mathit{H}_2CH_2NH$), 1.39 – 1.15 (m, 20H, CH_2), 0.84 (t, *J*= 6.1 Hz, 6H, CH_3). ^{31}P{^{1}H} NMR (162 MHz, DMSO-d_6): δ (ppm) -7.3. ^{19}F{^{1}H} NMR (377 MHz, DMSO-d_6): δ (ppm) -61.3. ^{13}C{^{1}H} NMR (101 MHz, DMSO-d_6) δ (ppm) 165.17 (C=O), 142.11 (d, *J*= 14.4 Hz, $C_{arom.}$-P), 140.75 ($C_{arom.}$), 135.20 ($C_{arom.}$), 135.14 (d, *J*= 12.3 Hz, $C_{arom.}$-P), 134.70 (d, *J*= 21.8 Hz, $CH_{arom.}$), 133.64 (d, *J*= 19.4 Hz, $CH_{arom.}$), 129.43-128.09 (m, $C_{arom.}$-CF_3), 129.00 ($CH_{arom.}$), 128.83 ($CH_{arom.}$),125.55-125.45 (m, $CH_{arom.}$), 124.03 (q, *J*= 272.3 Hz, CF_3), 120.65 (d, *J*= 8.1 Hz, $CH_{arom.}$), 39.38 (CH_2), 31.24 (CH_2), 29.00 (CH_2), 28.74 (CH_2), 28.65 (CH_2), 26.50 (CH_2), 22.07 (CH_2), 13.89 (CH_3). HRMS (ESI, m/z): Calculated for $C_{45}H_{52}F_6N_3O_3PH$, $[M+H]^+$ 828.3723, found: 828.3727. FT-IR (KBr plates, cm^{-1}): 696 (m), 830 (s), 1016 (w), 1060 (m), 1128 (m), 1168 (m), 1257 (m), 1292 (m), 1323 (s), 1395 (m), 1525 (m), 1590 (m), 1633 (m), 2853 (m), 2923 (m), 2953 (w), 3082 (w), 3248 (br).

Synthesis of BTA P^{CF3}

- Step 1: Synthesis of 4-(bis(3,5 bis(trifluoromethyl)phenyl)phosphino)aniline

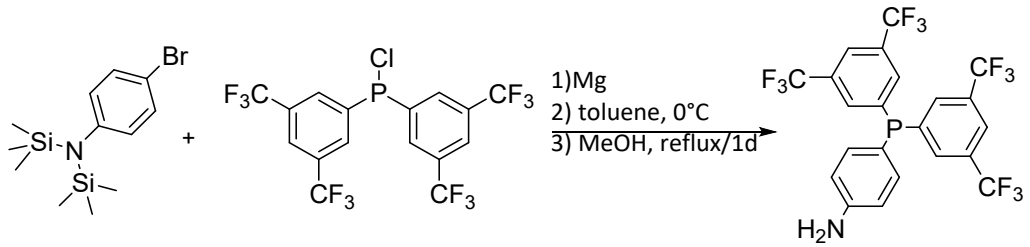

In a three-neck round-bottom flask equipped with a condenser under argon, 4-bromo-*N*,*N*-bis(trimethylsilyl)aniline (2.33 g, 7.38 mmol, 1.0 equiv.) in THF (7.4 mL) was added over 40 minutes to a well-stirred dispersion of magnesium turnings (0.21 g, 8.86 mmol, 1.2 equiv.) in a volume of THF sufficient to cover the magnesium turnings. Prior to starting the addition, magnesium turnings were activated with a small crystal of I_2 and one drop of 4-bromo-*N*,*N*-bis(trimethylsilyl)aniline. The reaction was stirred at room temperature, then heated to 60°C for 3 hours. THF was evaporated under vacuum and replaced by dry toluene. Bis(3,5-(trifluoromethyl)phenyl)chlorophosphine (4.0 g, 8.1 mmol, 1.1 equiv.) in dry toluene (7.4 mL) was added slowly over 45 minutes to the solution of 4-(*N*,*N*-trimethylsilyl)$_2$-aniline magnesium bromide while the reaction flask was cooled with in an ice bath. The reaction mixture was stirred at room temperature, and monitored by $^{31}P\{^1H\}$ NMR which showed full consumption of bis(3,5-(trifluoromethyl)phenyl)chlorophosphine after 1 h. The volatiles were removed under vacuum and the solid residue was extracted with dry Et_2O via a cannula to another three-neck round-bottom flask equipped with a special fritted funnel designed to perform filtrations under argon. Et_2O was removed under vacuum, the crude product was then dissolved in dry MeOH (22 mL) and the solution was stirred at reflux temperature for one day under argon. The solution was evaporated under vacuum, and the crude product was purified by flash column chromatography over silica gel, eluting with DCM/MeOH 99:1–95:5 gradient yielding 4-(bis(3,5 bis(trifluoromethyl)phenyl)phosphino)aniline (2.12 g, 52% yield) as a yellow oil. ^1H NMR (300 MHz, C_6D_6) δ (ppm) 7.76 (s, 2H), 7.59 (d, *J*= 6.4 Hz, 4H), 7.08 (t, *J*= 8.5 Hz, 2H), 6.63 (d, *J*= 7.5 Hz, 2H), 3.88 (br s, 2H, NH_2). $^{31}P\{^1H\}$ NMR (122 MHz, C_6D_6) δ (ppm) -4.69.

- Step 2: Synthesis of **BTA P^{CF3}**

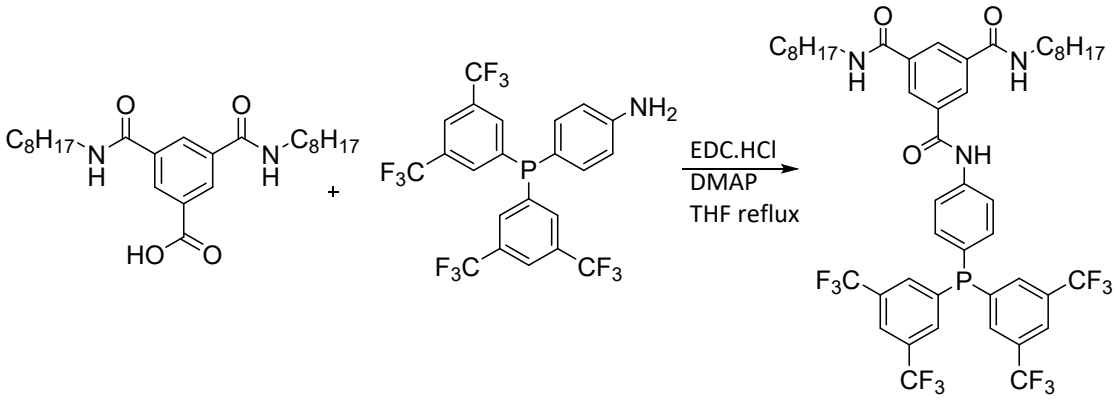

3,5-bisoctylaminocarbonyl-benzoic acid[12] (1.10 g, 2.59 mmol, 1.0 equiv.) was suspended in THF (100 mL) under argon and DMAP (0.46 g, 3.8 mmol, 1.5 equiv.), EDC·HCl (0.74 g, 3.8 mmol, 1.5 equiv.) and 4-(bis(3,5 bis(trifluoromethyl)phenyl)phosphino)aniline (2.0 g, 3.64 mmol, 1.4 equiv.) were added to the flask. The reaction mixture was stirred at reflux temperature for two days under argon. Then the reaction mixture was cooled to room temperature, and the solvent was evaporated under vacuum. The crude product was purified by flash column chromatography over silica gel, eluting with DCM/ethyl acetate 95:5–88:12 gradient, yielding **BTA P^{CF3}** (1.82 g, 73% yield) as a colorless solid. ^{1}H NMR (400 MHz, DMSO-d$_6$) δ (ppm) 10.73 (s, 1H, ArNH), 8.69 (t, *J*= 5.5 Hz, 2H, CH_2NH), 8.49 (s, 2H, BTA ring), 8.47 (s, 1H, BTA ring), 8.16 (s, 2H, PAr_2), 7.96 (d, *J*= 8.5 Hz, 2H, $CH_{arom.}$ linker), 7.89 (d, *J*= 6.4 Hz, 4H, PAr_2), 7.50 (t, *J*= 8.4 Hz, 2H, $CH_{arom.}$ linker), 3.29 (q, *J*= 6.1 Hz, 4H, CH_2NH), 1.57 – 1.50 (m, 4H, CH_2CH_2NH), 1.38 – 1.16 (m, 20H, CH_2), 0.82 (t, *J*= 7.2 Hz, 6H, CH_3). ^{31}P{^{1}H} NMR (122 MHz, DMSO-d$_6$) δ (ppm) -5.55. ^{19}F{^{1}H} NMR (377 MHz, DMSO-d$_6$): δ (ppm) –61.5. ^{13}C{^{1}H} NMR (101 MHz, DMSO-d$_6$) δ (ppm) 165.25 (C=O), 165.18 (C=O), 141.39 ($C_{arom.}$), 140.54 (d, *J*= 18.7 Hz, $C_{arom.}$-P), 135.24 ($C_{arom.}$), 135.17 (d, *J*= 22.1 Hz, $CH_{arom.}$), 135.02 ($C_{arom.}$), 133.09 (dd, *J*= 20.0 Hz, *J*=3.6 Hz $CH_{arom.}$), 130.71 (qd, *J*= 32.9 Hz, *J*=5.9 Hz $C_{arom.}$-CF_3), 129.08 ($CH_{arom.}$), 128.84 ($CH_{arom.}$), 126.83 (d, *J*= 9.3 Hz, $C_{arom.}$-P), 123.11 (t, *J*= 7.7 Hz, $CH_{arom.}$), 123.03 (q, *J*= 273.2 Hz, CF_3), 120.84 (d, *J*= 8.7 Hz, $CH_{arom.}$), 39.38 (CH_2), 31.24 (CH_2), 29.00 (CH_2), 28.74 (CH_2), 28.65 (CH_2), 26.50 (CH_2), 22.06 (CH_2), 13.83 (CH_3). HRMS (ESI, m/z): Calculated for $C_{47}H_{50}F_{12}N_3O_3PH$, $[M+H]^+$ 964.3471, found: 964.3479. FT-IR (KBr plates, cm^{-1}): 682 (s), 796 (m), 898 (m), 1112 (s), 1182 (m), 1272 (s), 1350 (m), 1525 (m), 1639 (m), 2854 (w), 2933 (w), 3080 (w), 3261 (br).

Selected ^{1}H NMR, MS and chiral HPLC analyses of catalytic samples

(*rac*)-DBA, synthesized by adapting literature procedures.[5,6]
^{1}H NMR (toluene-d_8), the sample contains *ca.* 30% of **Amine-DM** (signals at 7.90, 7.3-7.0, 6.19, 4.07 and 2.31 ppm)

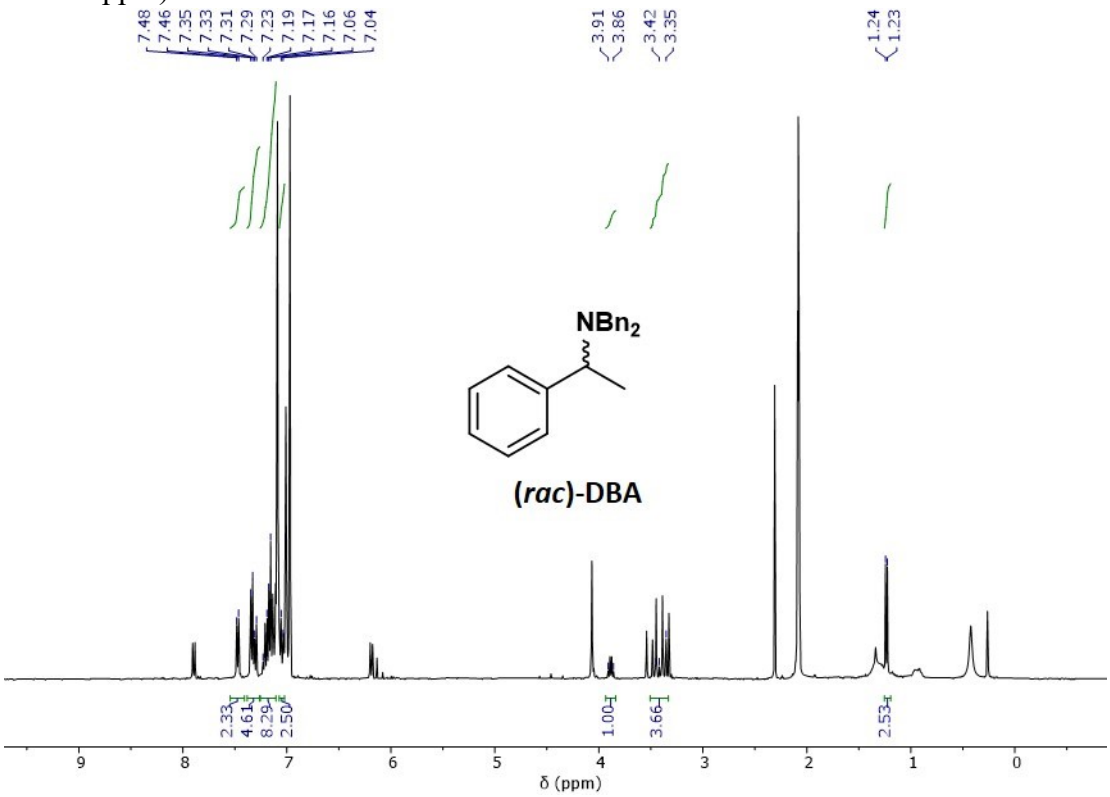

HPLC trace

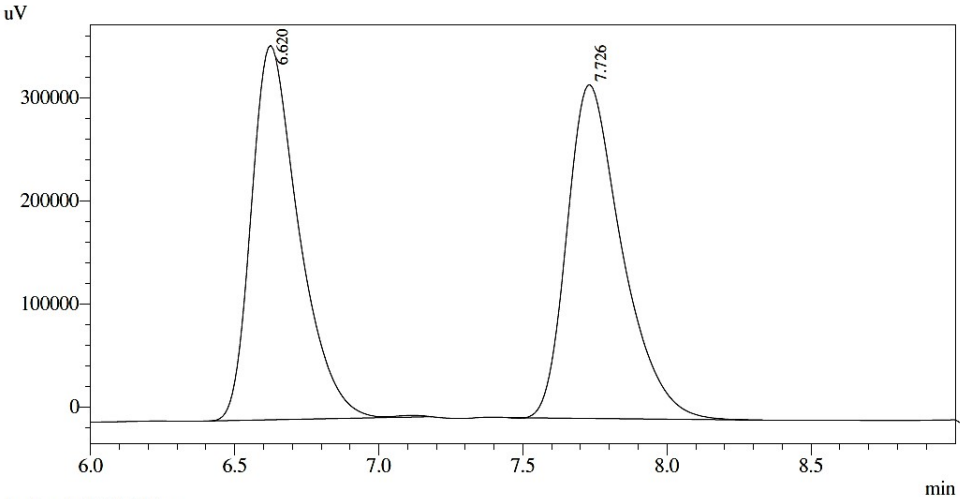

1 Det.A Ch1 / 230nm

<Results>

PeakTable

Detector A Ch1 230nm

Peak#	Ret. Time	Area	Area %
1	6.620	4166446	49.261
2	7.726	4291426	50.739
Total		8457872	100.000

Screening of the different BTA ligands [17 mM] with the initial conditions (Table 2):

BTA P^{CF3}

68% *e.e.* (*R*)-DBA

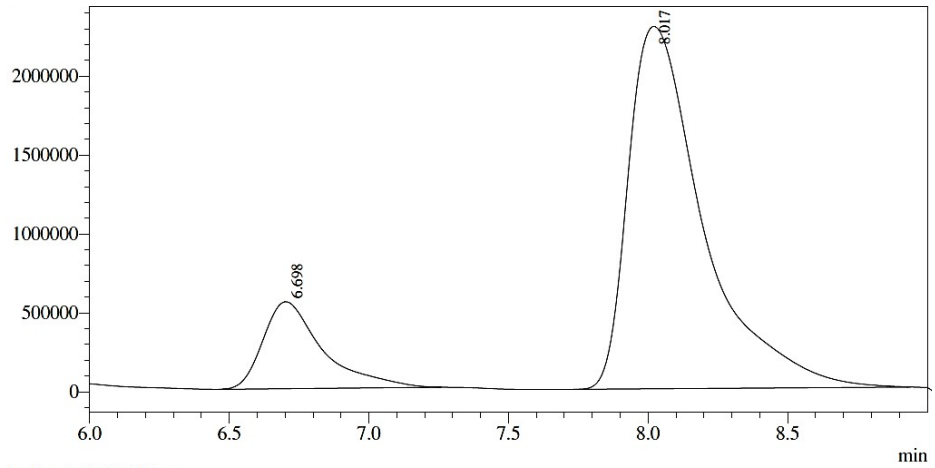

1 Det.A Ch1 / 230nm

<Results>

PeakTable

Detector A Ch1 230nm

Peak#	Ret. Time	Area	Area %
1	6.698	8144927	15.974
2	8.017	42843346	84.026
Total		50988273	100.000

BTA P^{Me}

58% *e.e.* (*R*)-DBA

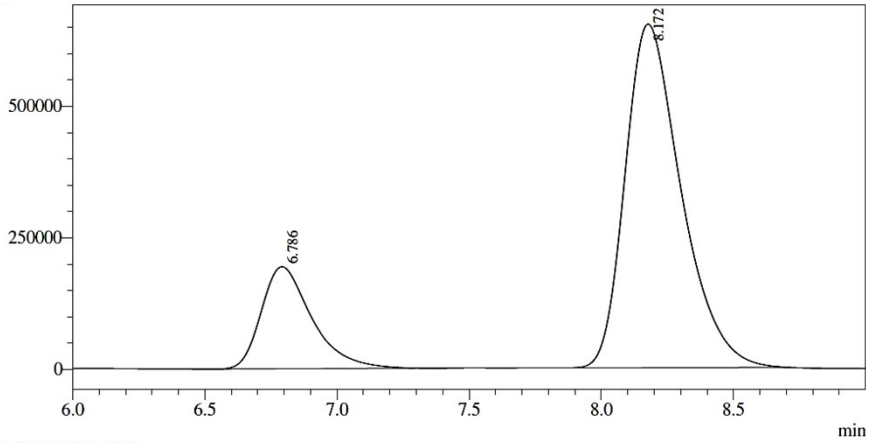

1 Det.A Ch1 / 230nm
2 Det.A Ch2 / 230nm

<Results>

PeakTable

Detector A Ch1 230nm

Peak#	Ret. Time	Area	Area %
1	6.786	2575140	21.104
2	8.172	9627198	78.896
Total		12202338	100.000

BTA P*p*-F

19% *e.e.* (*R*)-DBA

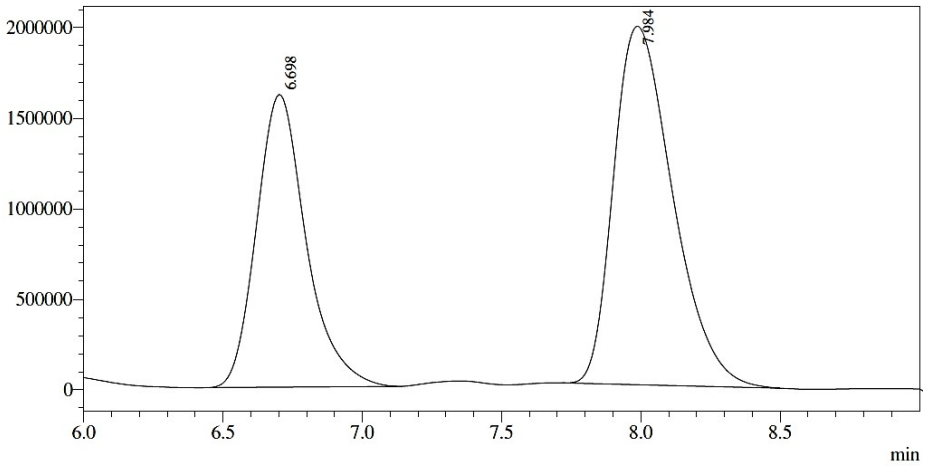

1 Det.A Ch1 / 230nm

<Results>

PeakTable

Detector A Ch1 230nm

Peak#	Ret. Time	Area	Area %
1	6.698	20004374	40.587
2	7.984	29283559	59.413
Total		49287933	100.000

BTA P*p*-CF3

7% *e.e.* (*R*)-DBA

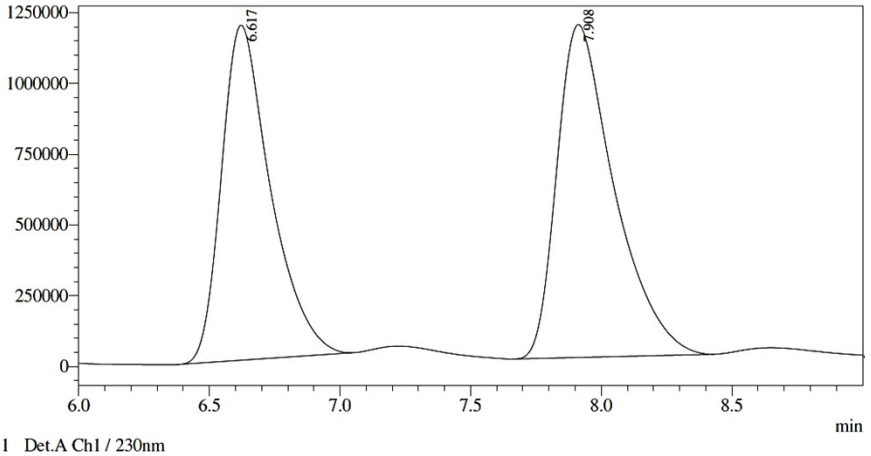

1 Det.A Ch1 / 230nm

<Results>

PeakTable

Detector A Ch1 230nm

Peak#	Ret. Time	Area	Area %
1	6.617	15487024	46.292
2	7.908	17968269	53.708
Total		33455293	100.000

BTA P^{H}
29% *e.e.* (*R*)-DBA

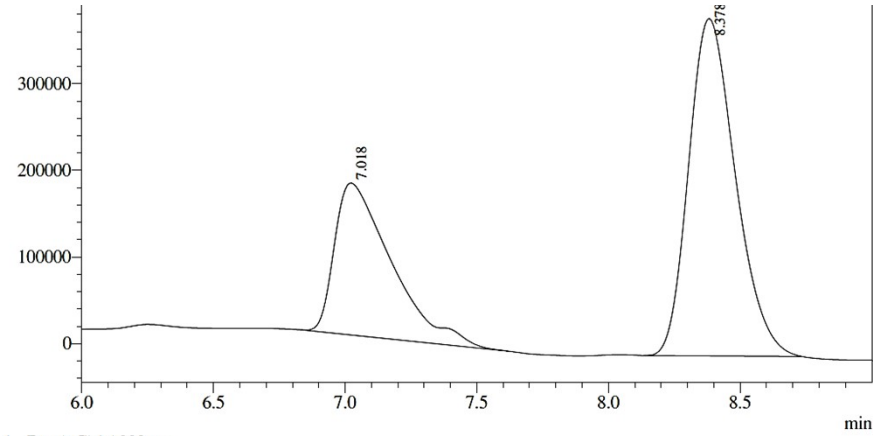

1 Det.A Ch1 / 230nm

<Results>

PeakTable

Detector A Ch1 230nm

Peak#	Ret. Time	Area	Area %
1	7.018	2629074	35.342
2	8.378	4809844	64.658
Total		7438918	100.000

Optimization reactions with **BTA P^{CF3}** [*x* mM] and **(*R*)-BTA** (f_s^0= 50%) – Tables 3 and S1.1-S1.5:

BTA P^{CF3} [17 mM], [$Cu(OAc)_2$] (5 mol%), DMMS (400 mol%), Amine-DM (120 mol%), **313 K**
73% *e.e.* (*R*)-DBA

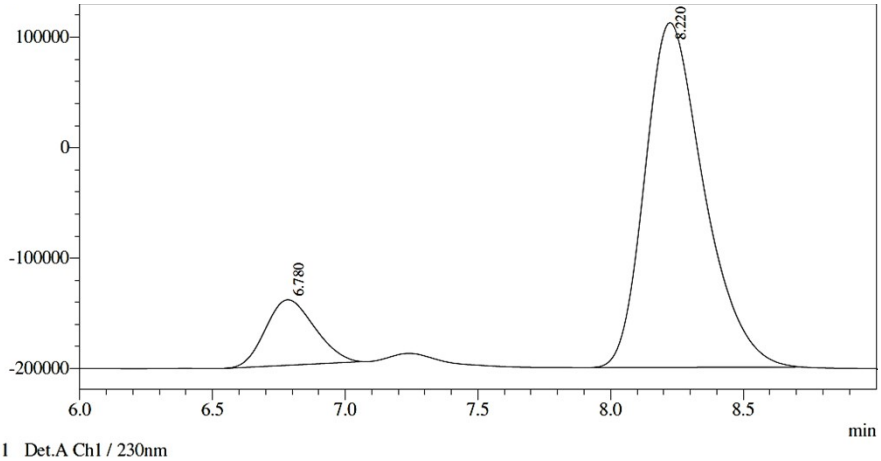

1 Det.A Ch1 / 230nm

<Results>

PeakTable

Detector A Ch1 230nm

Peak#	Ret. Time	Area	Area %
1	6.780	766011	13.669
2	8.220	4838174	86.331
Total		5604185	100.000

BTA P^{CF3} [17 mM], [$Cu(OAc)_2$] (5 mol%), DMMS (400 mol%), Amine-DM (120 mol%), **333 K**
63% *e.e.* (*R*)-DBA

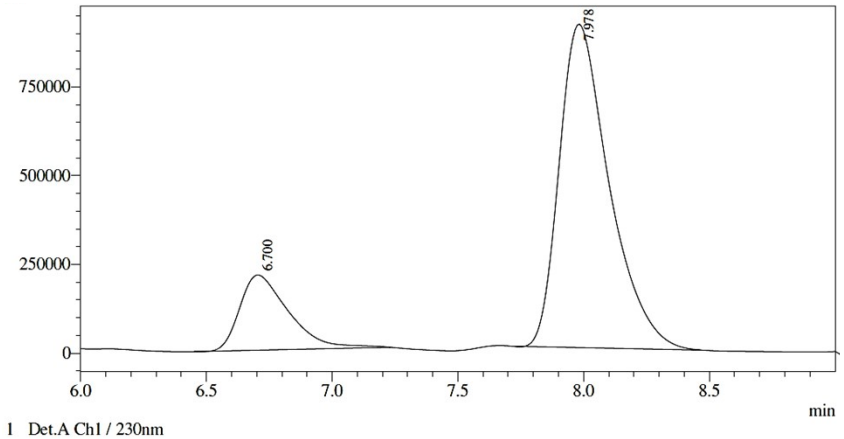

1 Det.A Ch1 / 230nm

<Results>

PeakTable

Detector A Ch1 230nm

Peak#	Ret. Time	Area	Area %
1	6.700	2855889	18.505
2	7.978	12576978	81.495
Total		15432868	100.000

BTA P^{CF3} [17 mM], **[$Cu(CO_2$*i*-Pr$)_2$]** (5 mol%), DMMS (400 mol%), Amine-DM (120 mol%), 313 K
67% *e.e.* (*R*)-DBA

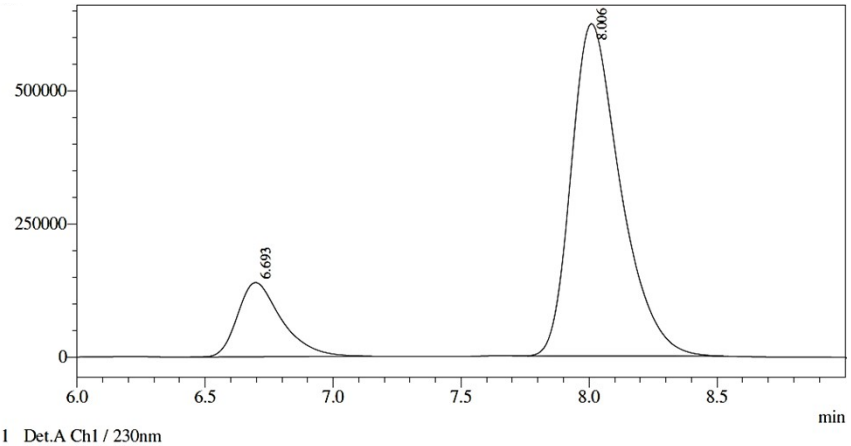

1 Det.A Ch1 / 230nm

<Results>

PeakTable

Detector A Ch1 230nm

Peak#	Ret. Time	Area	Area %
1	6.693	1672074	16.657
2	8.006	8365991	83.343
Total		10038064	100.000

BTA P^{CF3} [10 mM], [$Cu(OAc)_2$] (5 mol%), DMMS (400 mol%), Amine-DM (120 mol%), 313 K
66% *e.e.* (*R*)-DBA

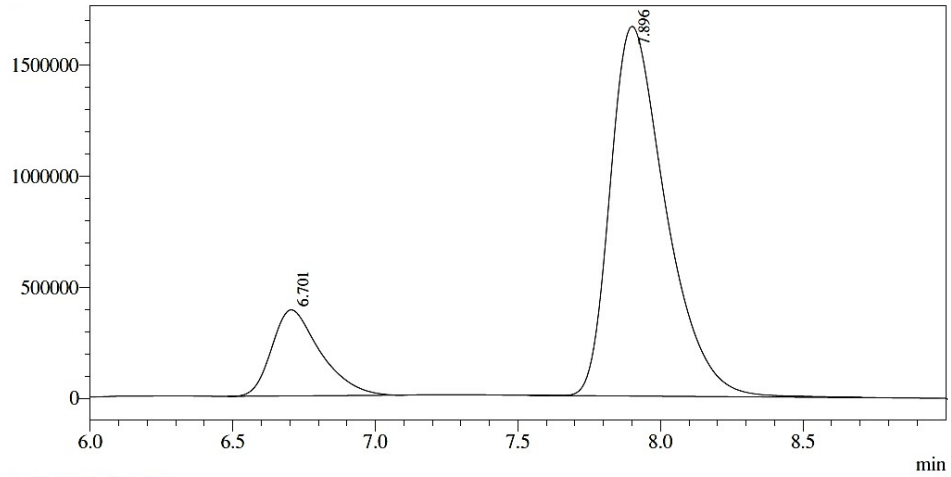

1 Det.A Ch1 / 230nm

<Results>

PeakTable

Detector A Ch1 230nm

Peak#	Ret. Time	Area	Area %
1	6.701	4587396	16.899
2	7.896	22558728	83.101
Total		27146123	100.000

BTA P^{CF3} [5 mM], [$Cu(OAc)_2$] (5 mol%), DMMS (400 mol%), Amine-DM (120 mol%), 313 K
66% *e.e.* (*R*)-DBA

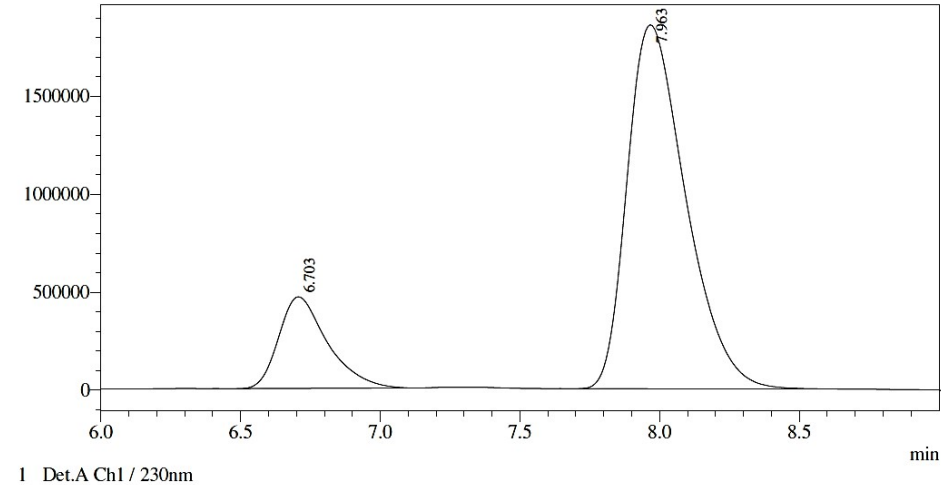

1 Det.A Ch1 / 230nm

<Results>

PeakTable

Detector A Ch1 230nm

Peak#	Ret. Time	Area	Area %
1	6.703	5666406	17.264
2	7.963	27155571	82.736
Total		32821978	100.000

BTA P^{CF3} [2.5 mM], [$Cu(OAc)_2$] (5 mol%), DMMS (400 mol%), Amine-DM (120 mol%), 313 K
65% *e.e.* (*R*)-DBA

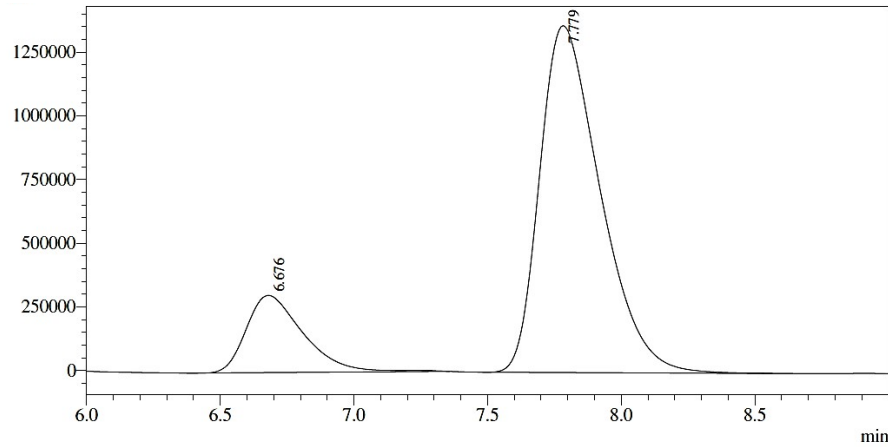

1 Det.A Ch1 / 230nm

<Results>

PeakTable

Detector A Ch1 230nm

Peak#	Ret. Time	Area	Area %
1	6.676	4486547	17.334
2	7.779	21396663	82.666
Total		25883210	100.000

BTA P^{CF3} [17 mM], [$Cu(OAc)_2$] (5 mol%), DMMS (400 mol%), Amine-DM (**180 mol%**), 313 K
69% *e.e.* (*R*)-DBA

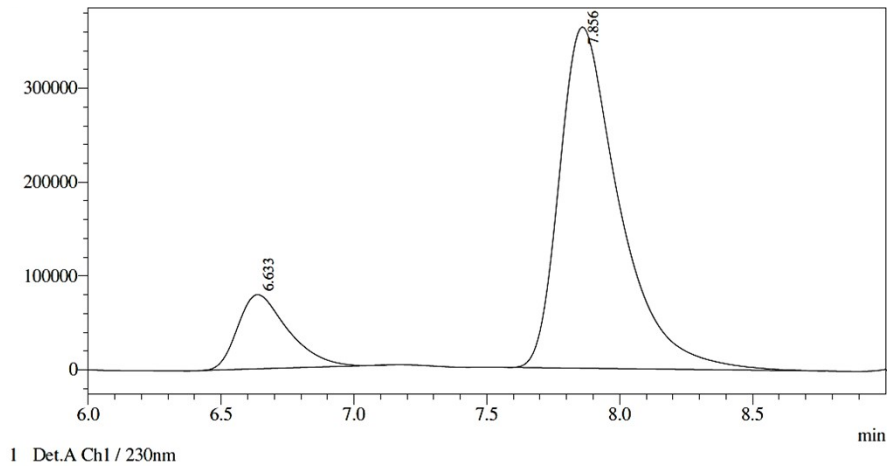

1 Det.A Ch1 / 230nm

<Results>

PeakTable

Detector A Ch1 230nm

Peak#	Ret. Time	Area	Area %
1	6.633	1038963	15.408
2	7.856	5704070	84.592
Total		6743033	100.000

BTA P^{CF3} [17 mM], **(*S*)-BTA**, [$Cu(OAc)_2$] (5 mol%), DMMS (400 mol%), Amine-DM (**180 mol%**), 313 K
69% *e.e.* (*S*)-DBA

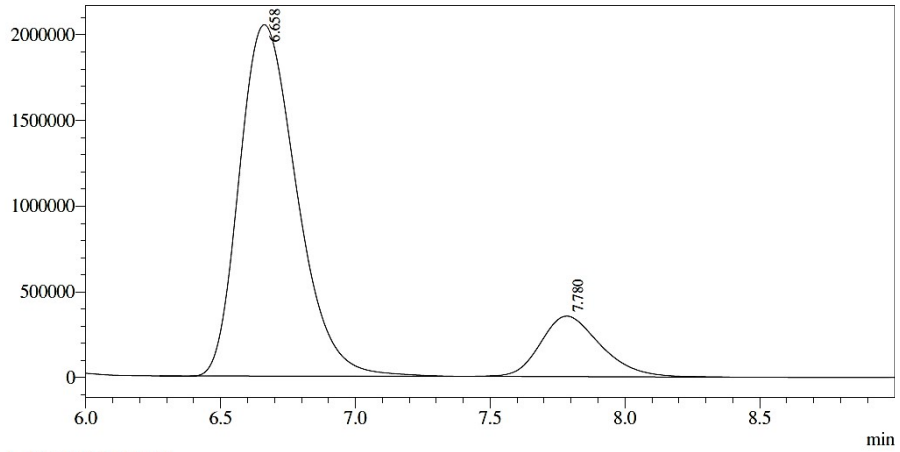

1 Det.A Ch1 / 230nm

<Results>

PeakTable

Detector A Ch1 230nm

Peak#	Ret. Time	Area	Area %
1	6.658	30310500	84.702
2	7.780	5474257	15.298
Total		35784757	100.000

Optimization reactions with **$BTAP^{Me}$** [17 mM] and **(*R*)-BTA** (f_s^0= 50%) – Table S2

BTA P^{Me} [17 mM], DMMS (400 mol%), Amine-DM (120 mol%), **313 K**
57% *e.e.* (*R*)-DBA

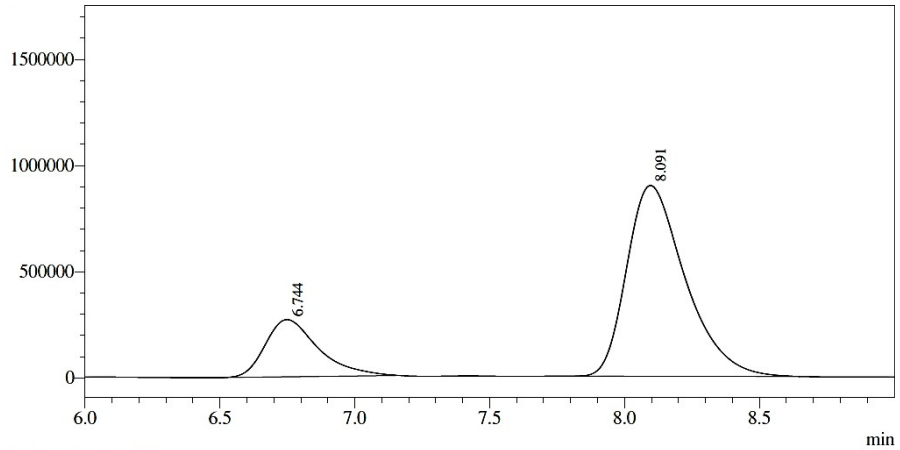

1 Det.A Ch1 / 230nm
2 Det.A Ch2 / 230nm

<Results>

PeakTable

Detector A Ch1 230nm

Peak#	Ret. Time	Area	Area %
1	6.744	3691456	21.395
2	8.091	13562513	78.605
Total		17253969	100.000

Isolated yield (60%) under optimized conditions (**BTA P^{CF3}** [18 mM]):

BTA P^{CF3} [18 mM], **(*S*)-BTA**, [$Cu(OAc)_2$] (5 mol%), DMMS (400 mol%), Amine-DM (180 mol%), 313 K

^{1}H NMR (toluene-d_8)

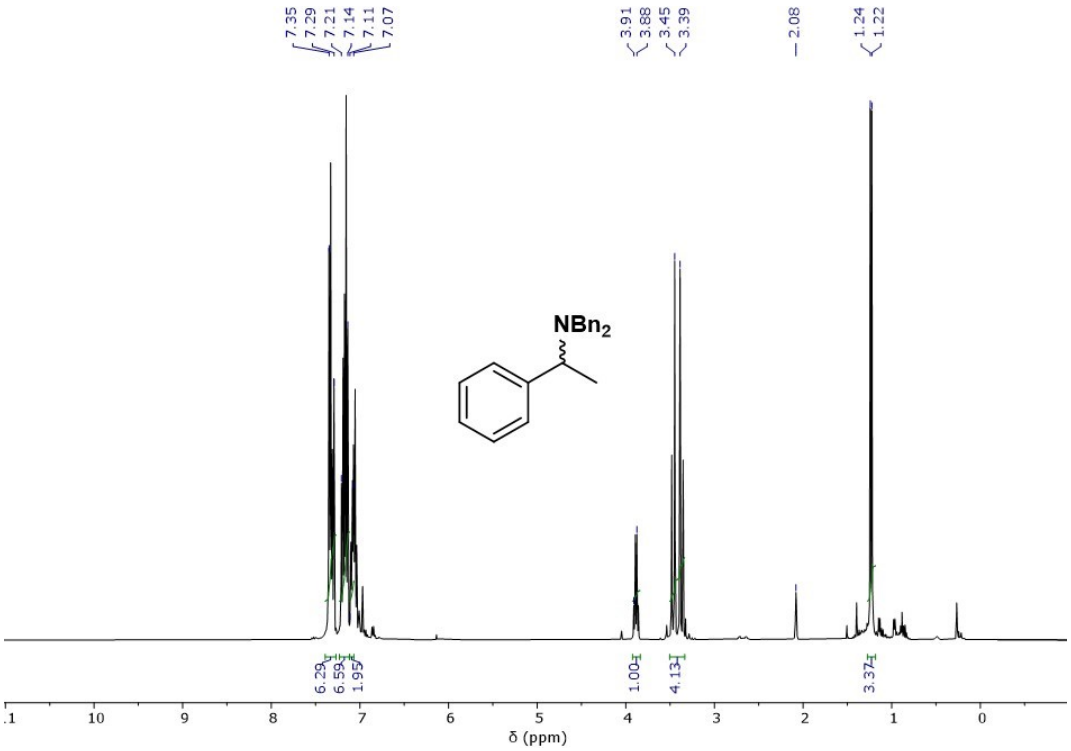

HPLC trace, **64% *e.e.* (*S*)-DBA**

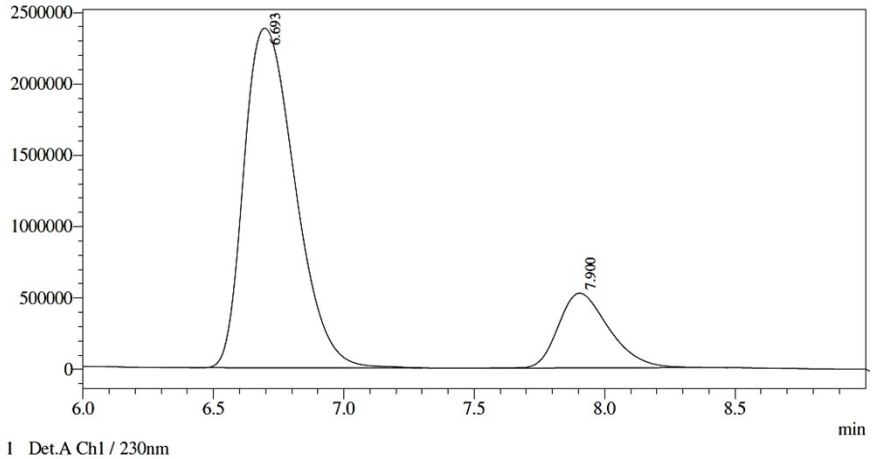

1 Det.A Ch1 / 230nm

<Results>

PeakTable

Detector A Ch1 230nm

Peak#	Ret. Time	Area	Area %
1	6.693	32387215	82.069
2	7.900	7076207	17.931
Total		39463422	100.000

Sergeants-and-soldiers experiments with **BTA P^{CF3}** [10 mM] and **(*S*)-BTA**: In presence of **a-BTA** – Table S3:

(*S*)-BTA [0.05 mM], f_s^0= 0.25%
42% *e.e.* (*S*)-DBA

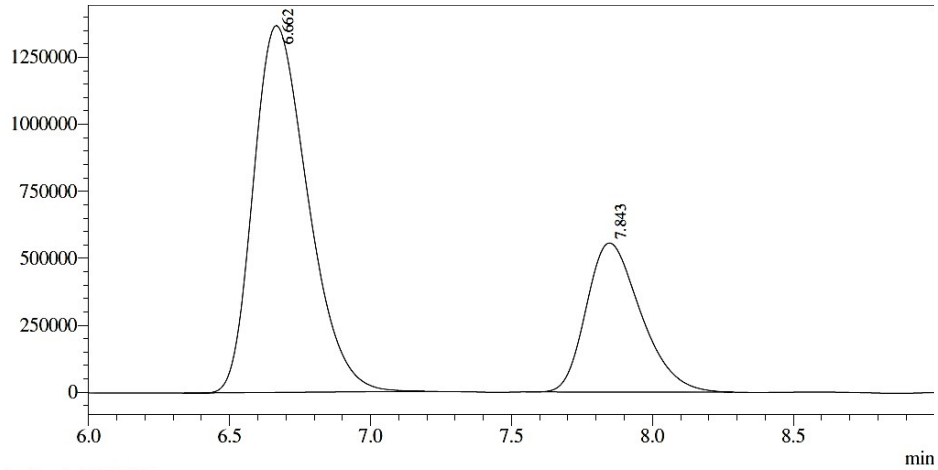

1 Det.A Ch1 / 230nm

<Results>

PeakTable

Detector A Ch1 230nm

Peak#	Ret. Time	Area	Area %
1	6.662	18355607	71.020
2	7.843	7490138	28.980
Total		25845745	100.000

(*S*)-BTA [0.10 mM], f_s^0= 0.50%
52% *e.e.* (*S*)-DBA

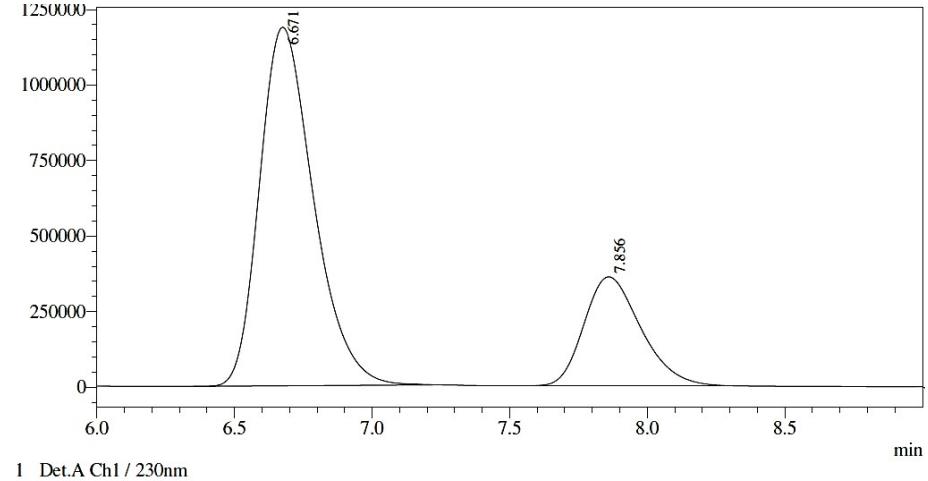

1 Det.A Ch1 / 230nm

<Results>

PeakTable

Detector A Ch1 230nm

Peak#	Ret. Time	Area	Area %
1	6.671	16168657	75.837
2	7.856	5151756	24.163
Total		21320413	100.000

(*S*)-BTA [0.19 mM], f_s^0= 1.0%

62% *e.e.* (*S*)-DBA

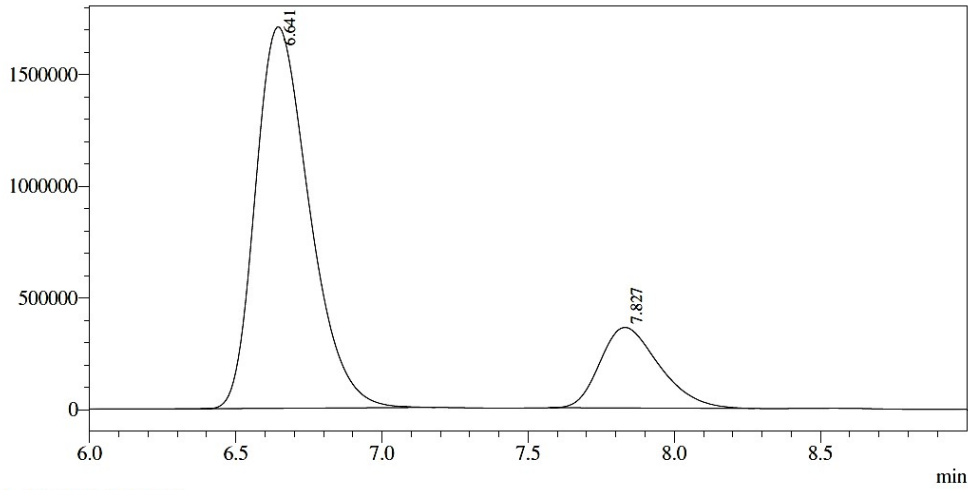

1 Det.A Ch1 / 230nm

<Results>

PeakTable

Detector A Ch1 230nm

Peak#	Ret. Time	Area	Area %
1	6.641	21888357	81.144
2	7.827	5086406	18.856
Total		26974763	100.000

(*S*)-BTA [0.50 mM], f_s^0= 2.5%

75% *e.e.* (*S*)-DBA

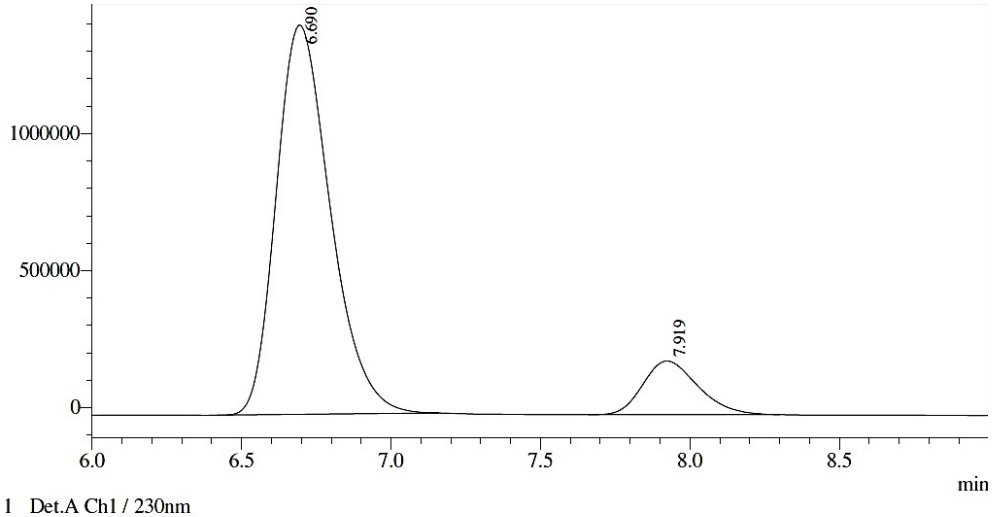

1 Det.A Ch1 / 230nm

<Results>

PeakTable

Detector A Ch1 230nm

Peak#	Ret. Time	Area	Area %
1	6.690	17892179	87.706
2	7.919	2508013	12.294
Total		20400191	100.000

(*S*)-BTA [1.0 mM], f_s^0= 5.0%
77% *e.e.* (*S*)-DBA

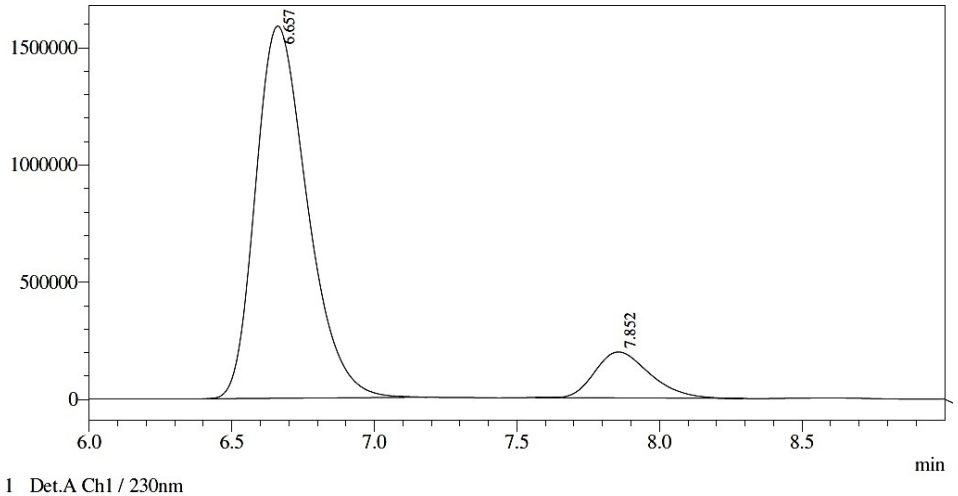

1 Det.A Ch1 / 230nm

<Results>

PeakTable

Detector A Ch1 230nm

Peak#	Ret. Time	Area	Area %
1	6.657	20024596	88.410
2	7.852	2625208	11.590
Total		22649804	100.000

(*S*)-BTA [2.1 mM], f_s^0= 10.0%
81% *e.e.* (*S*)-DBA

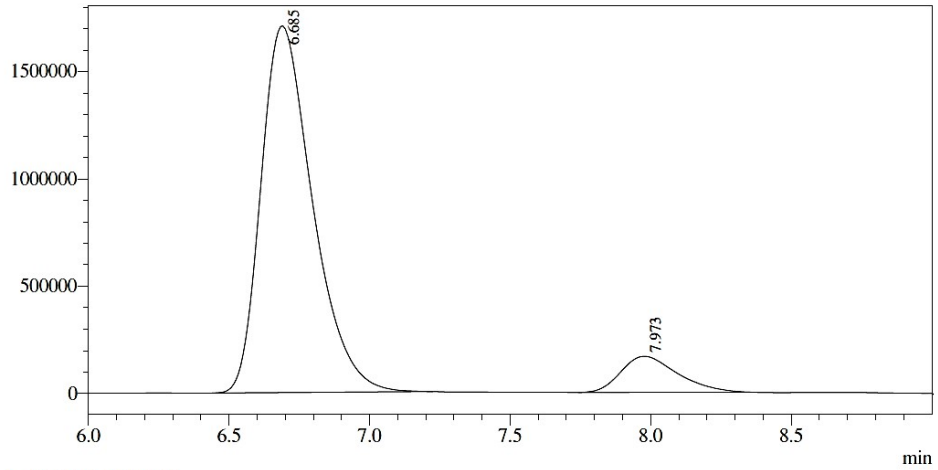

1 Det.A Ch1 / 230nm

<Results>

PeakTable

Detector A Ch1 230nm

Peak#	Ret. Time	Area	Area %
1	6.685	21813893	90.261
2	7.973	2353805	9.739
Total		24167698	100.000

(*S*)-BTA [6.4 mM], f_s^0= 25.0%
81% *e.e.* (*S*)-DBA

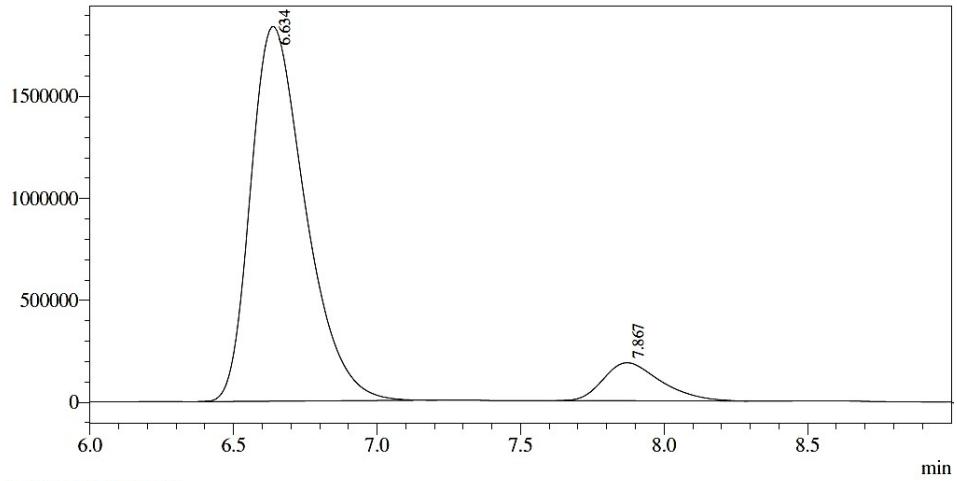

1 Det.A Ch1 / 230nm

<Results>

PeakTable

Detector A Ch1 230nm

Peak#	Ret. Time	Area	Area %
1	6.634	24318173	90.371
2	7.867	2591147	9.629
Total		26909320	100.000

(*S*)-BTA [18.9 mM], f_s^0= 50.0%
81% *e.e.* (*S*)-DBA

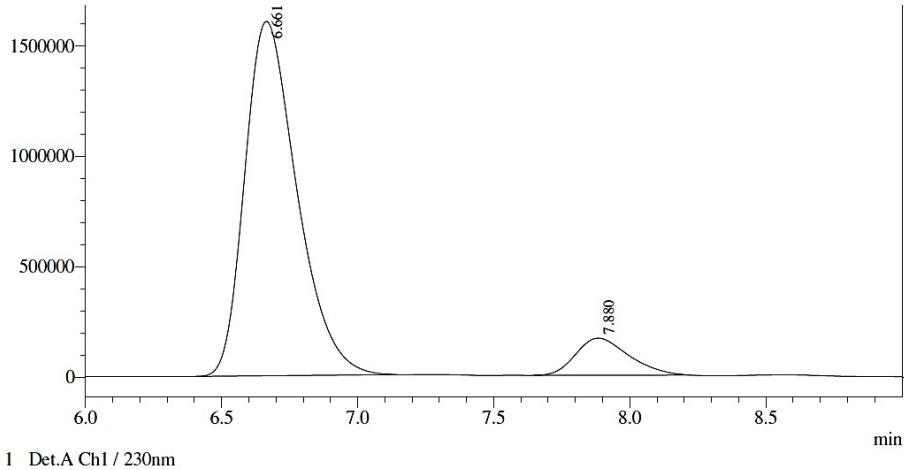

1 Det.A Ch1 / 230nm

<Results>

PeakTable

Detector A Ch1 230nm

Peak#	Ret. Time	Area	Area %
1	6.661	21398887	90.379
2	7.880	2277914	9.621
Total		23676801	100.000

Sergeants-and-soldiers experiments with **BTA P^{CF3}** [10 mM] and **(*S*)-BTA**: In absence of **a-BTA** – Table S3

(*S*)-BTA [0.1 mM], f_s^0= 1.0%
10% *e.e.* (*S*)-DBA

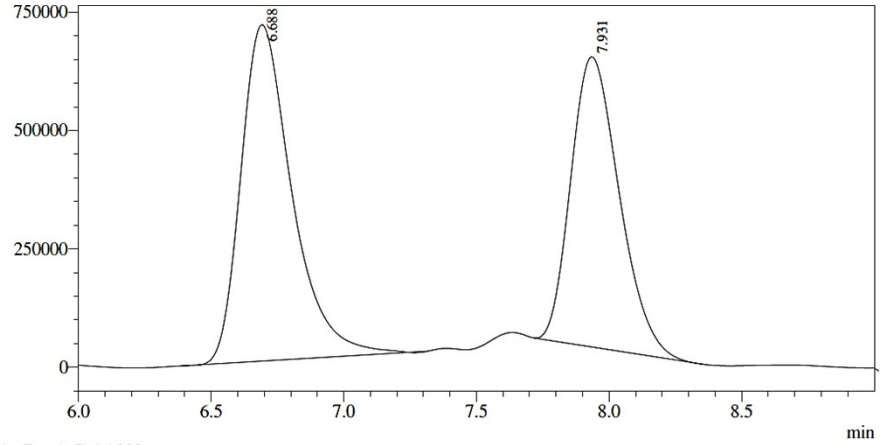

1 Det.A Ch1 / 230nm

<Results>

PeakTable

Detector A Ch1 230nm

Peak#	Ret. Time	Area	Area %
1	6.688	9503172	54.946
2	7.931	7792153	45.054
Total		17295325	100.000

(*S*)-BTA [9.6 mM], f_s^0= 50%
70% *e.e.* (*S*)-DBA

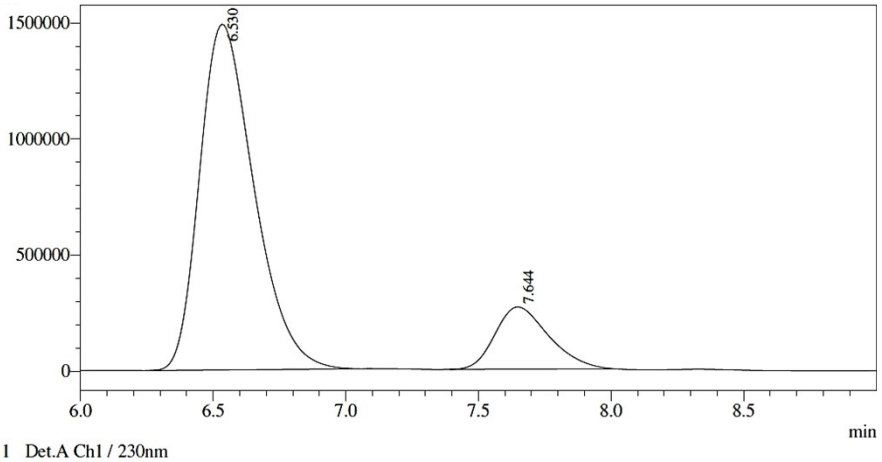

1 Det.A Ch1 / 230nm

<Results>

PeakTable

Detector A Ch1 230nm

Peak#	Ret. Time	Area	Area %
1	6.530	21276219	84.917
2	7.644	3778960	15.083
Total		25055178	100.000

ESI-MS analysis of the reaction mixture corresponding to Figure S10.

Full spectrum:

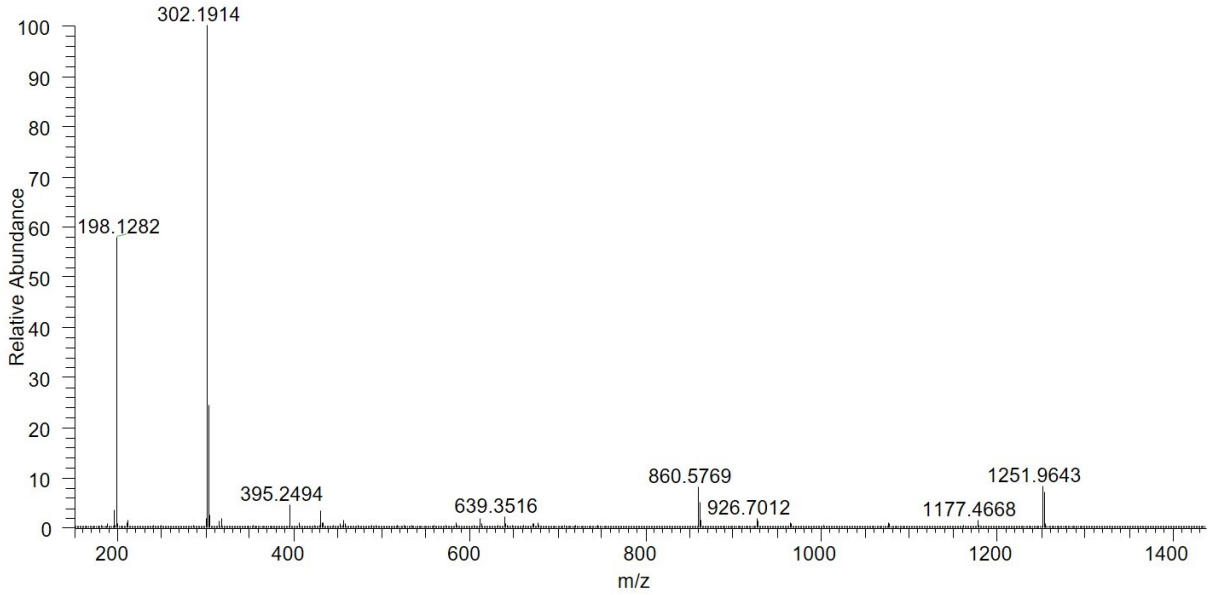

Identified species:

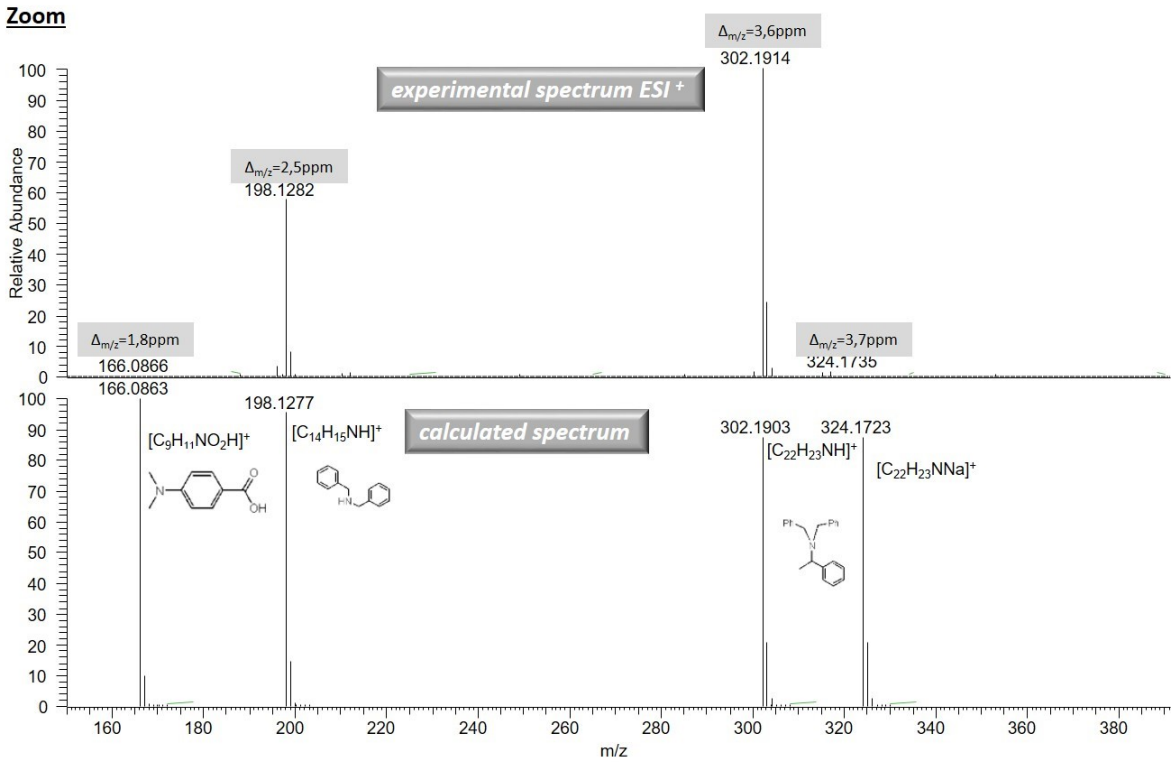

NMR spectra

BTA P$^{p\text{-F}}$

^{1}H NMR (DMSO-d$_6$)

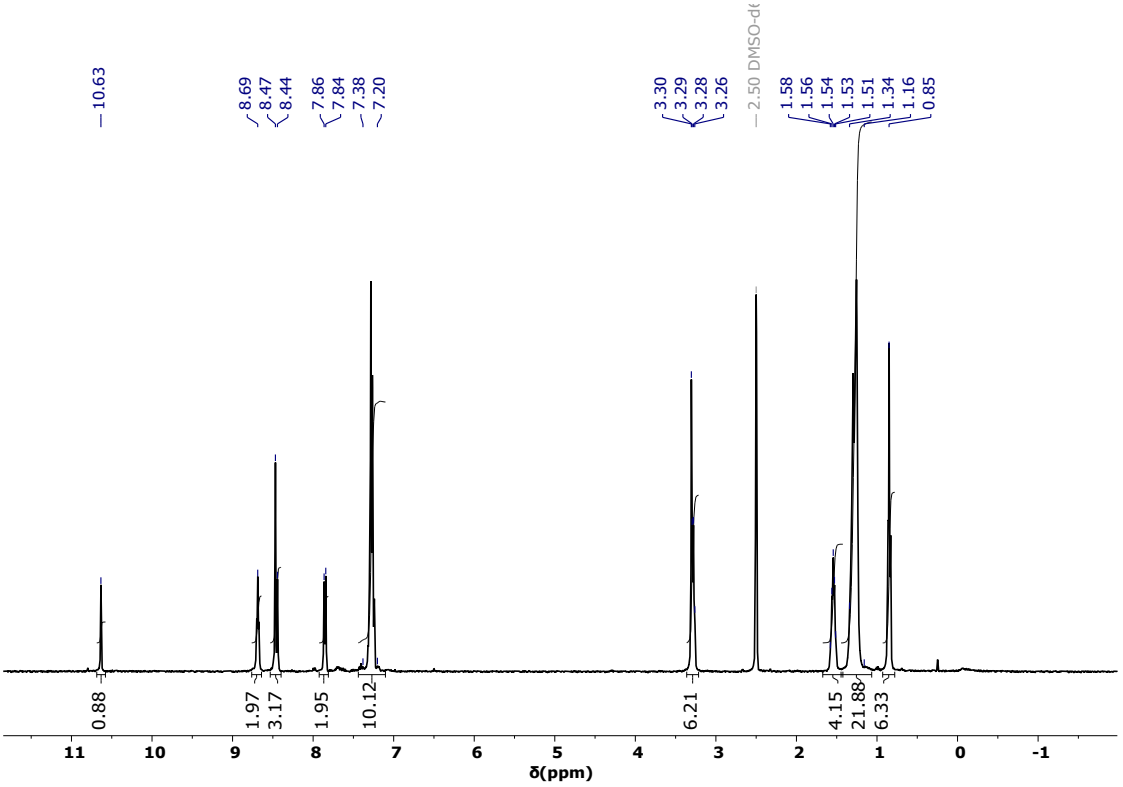

^{31}P{^{1}H} NMR (DMSO-d$_6$)

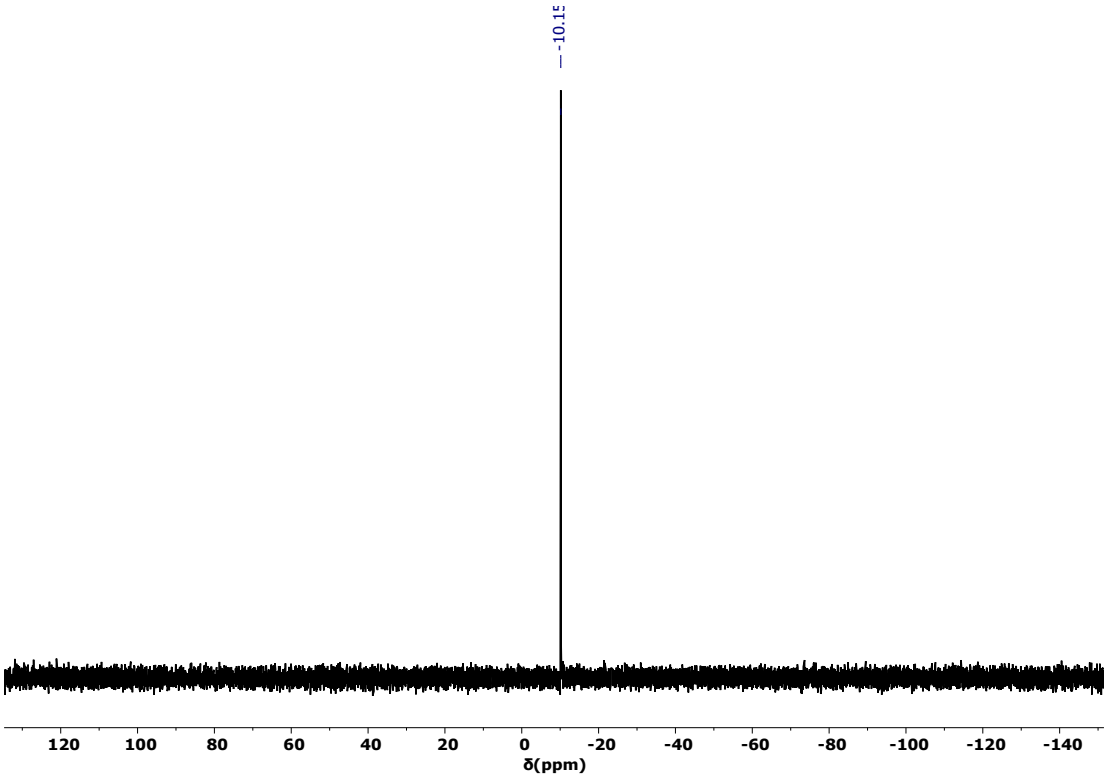

$^{19}F\{^{1}H\}$ NMR (DMSO-d_6)

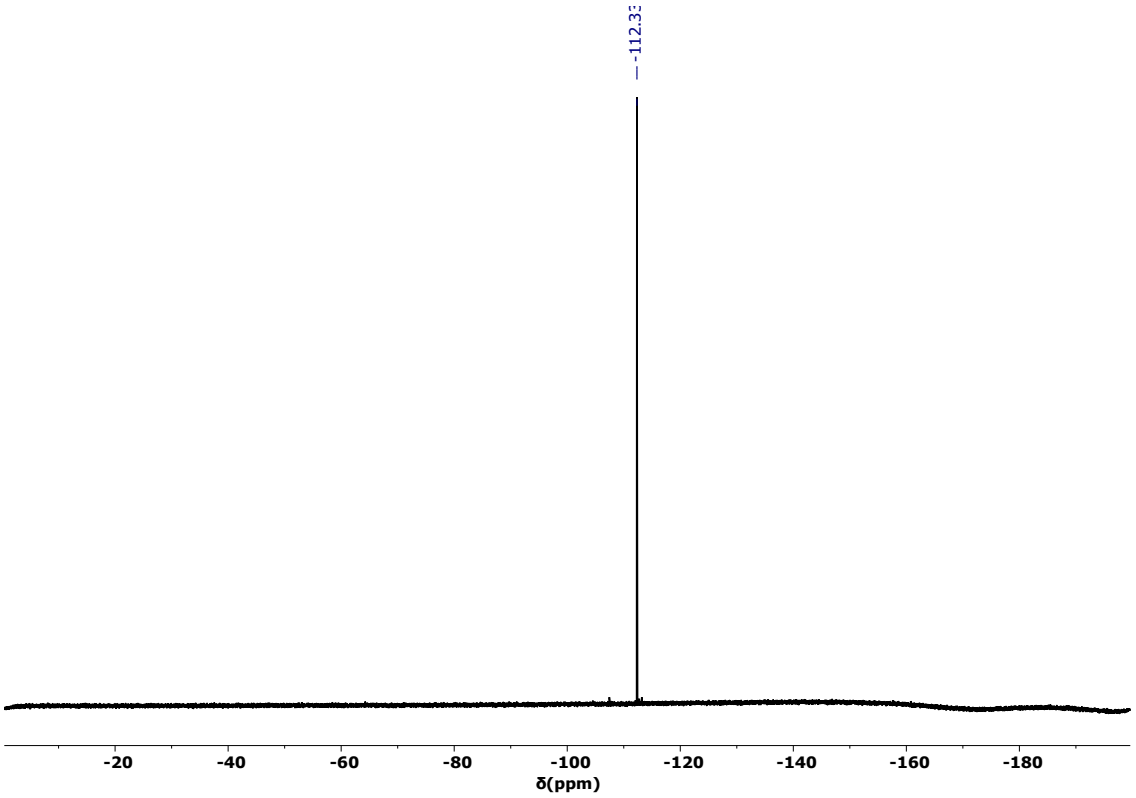

$^{13}C\{^{1}H\}$ NMR (DMSO-d_6) DEPT135

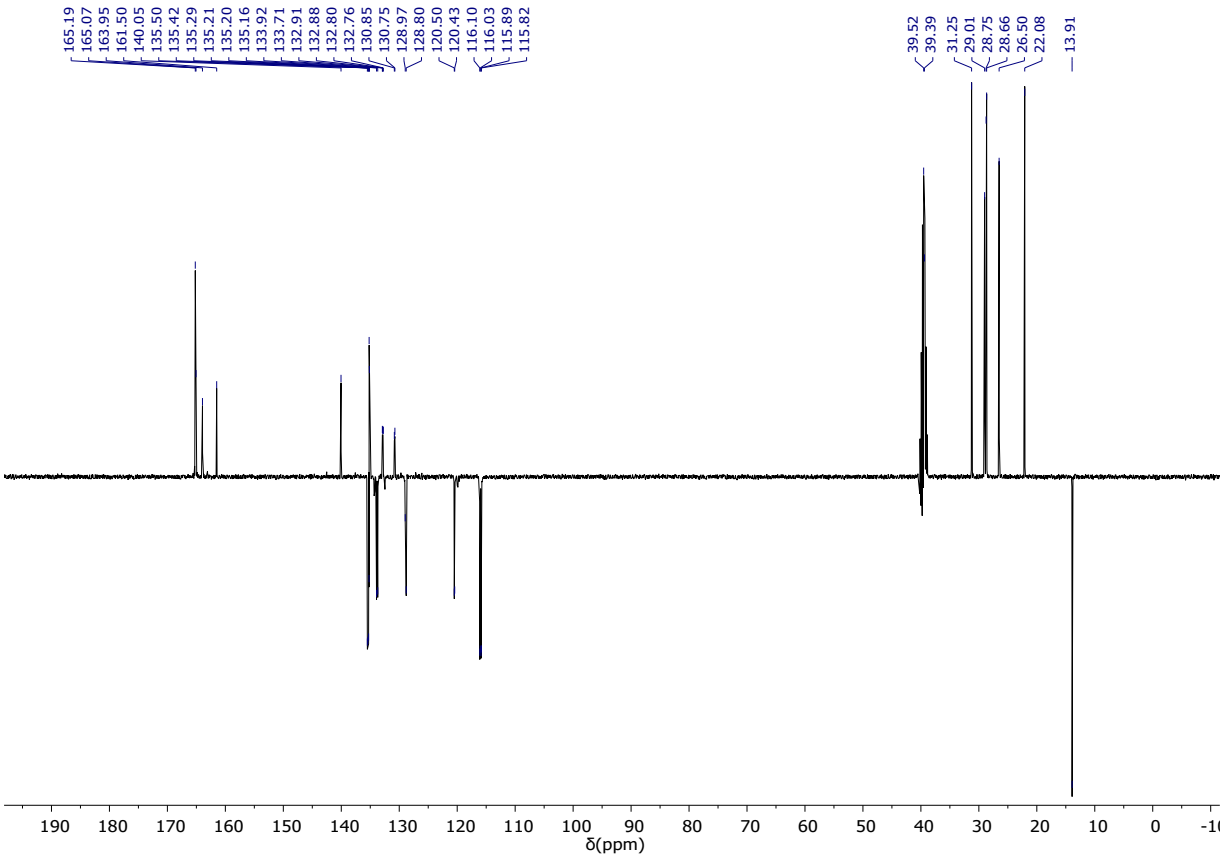

BTA P*p*-CF3

^{1}H NMR (DMSO-d_6)

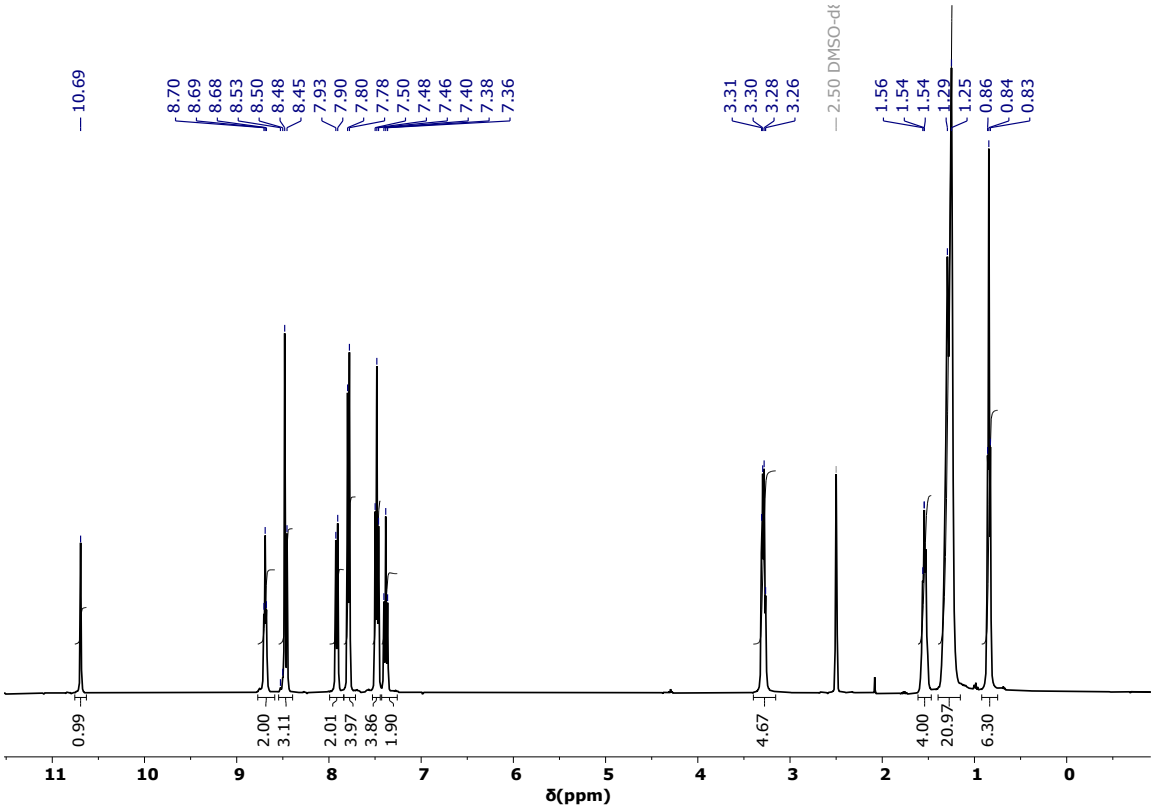

^{31}P{^{1}H} NMR (DMSO-d_6)

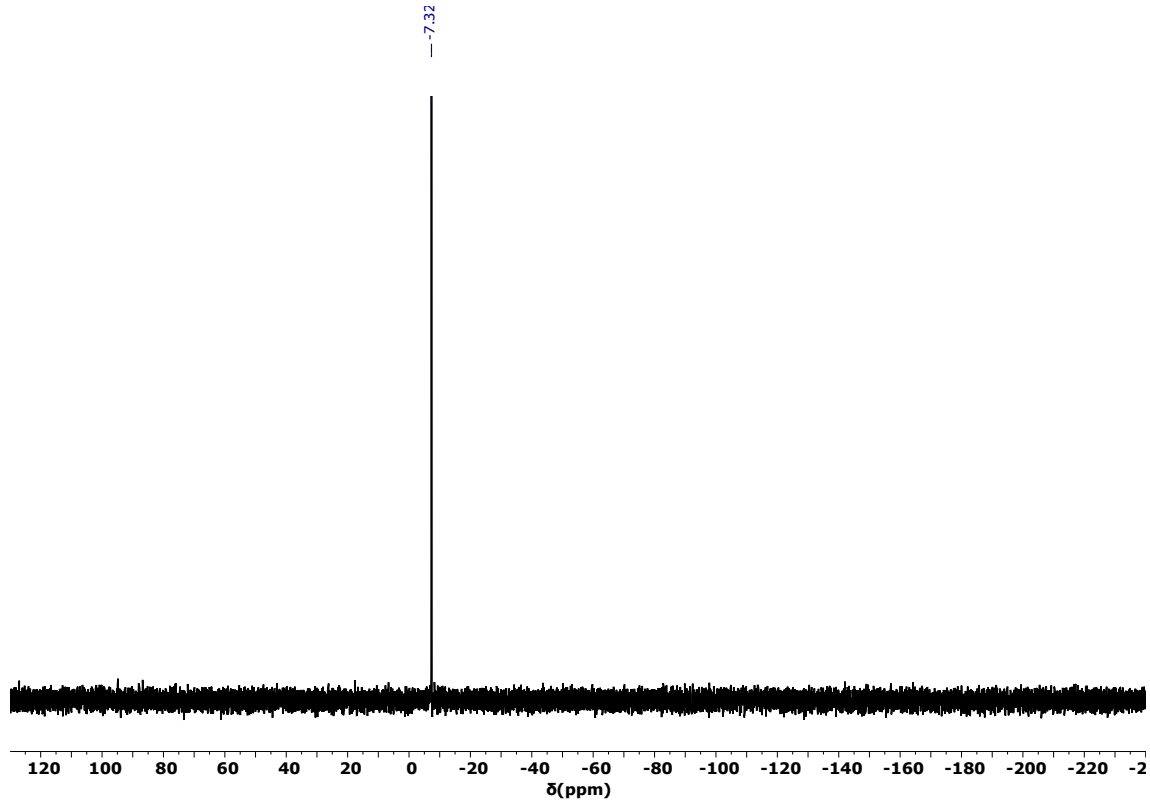

$^{19}F\{^{1}H\}$ NMR (DMSO-d_6)

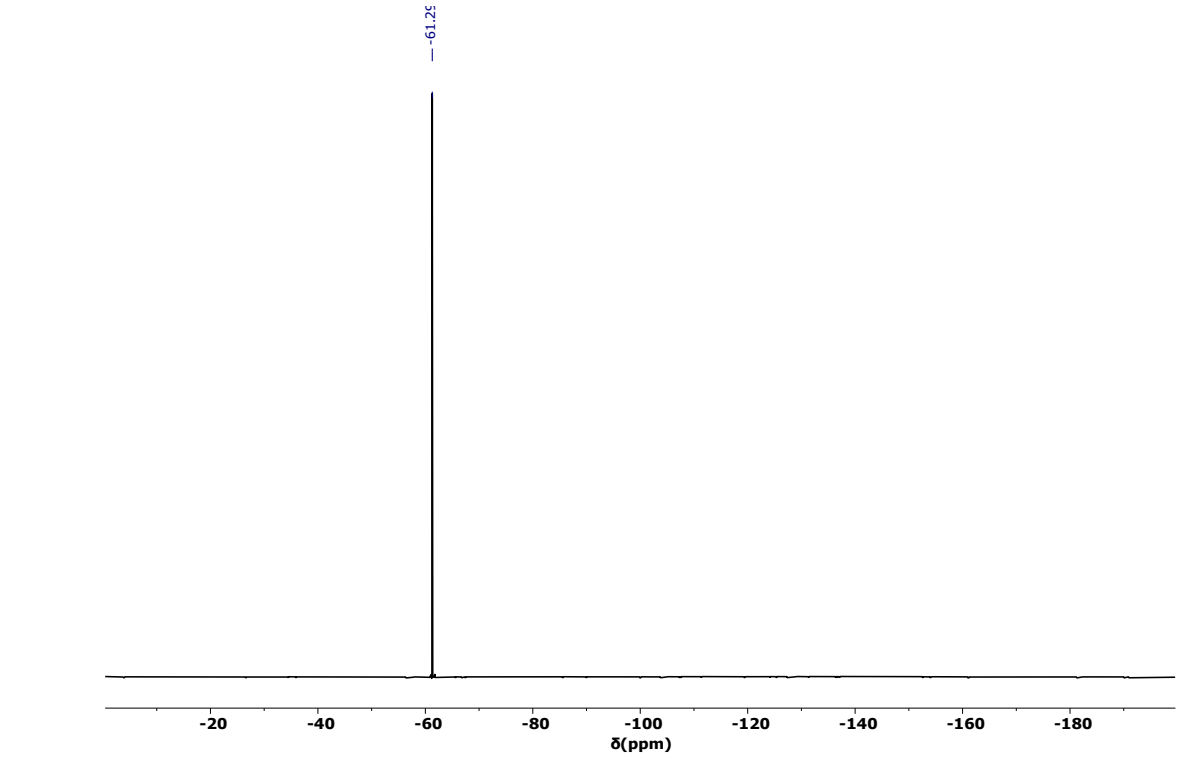

$^{13}C\{^{1}H\}$ NMR (DMSO-d_6) DEPT135

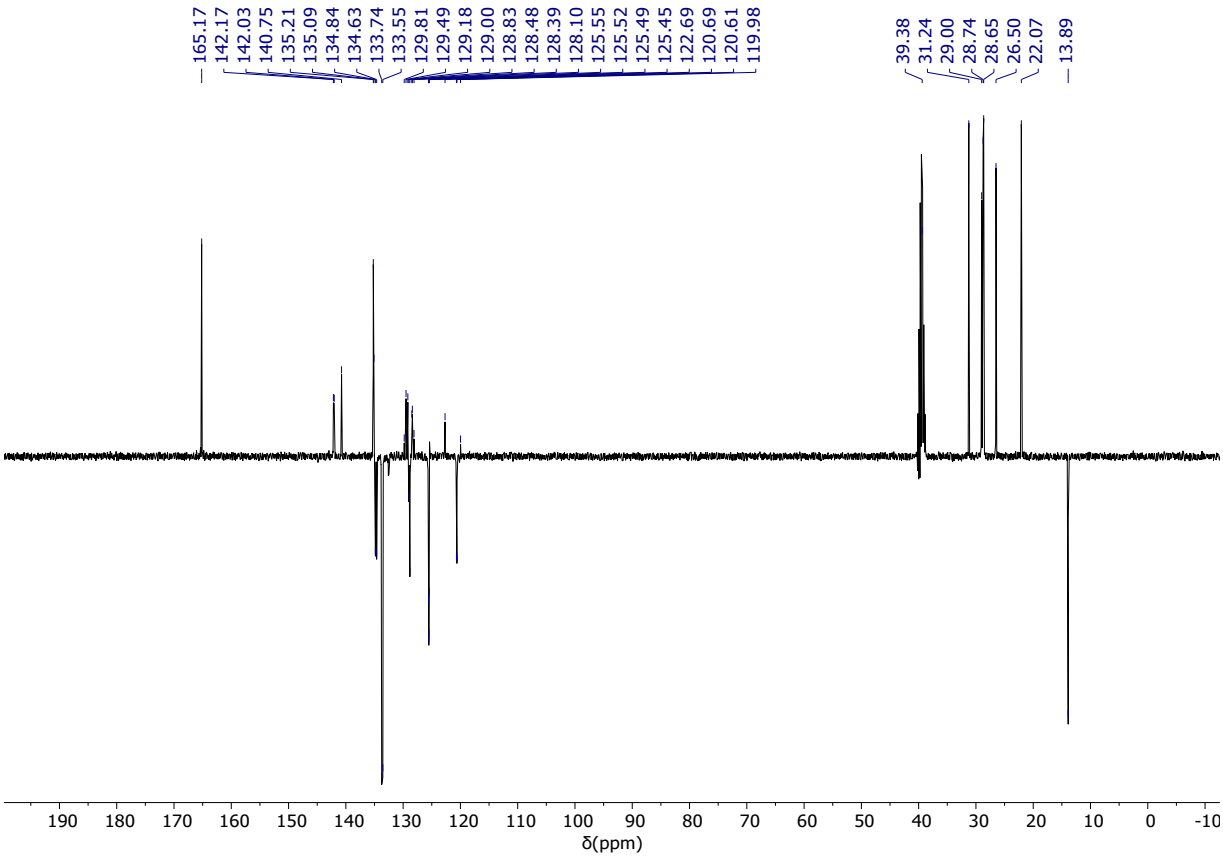

BTA P^{CF3}

^{1}H NMR (DMSO-d_6)

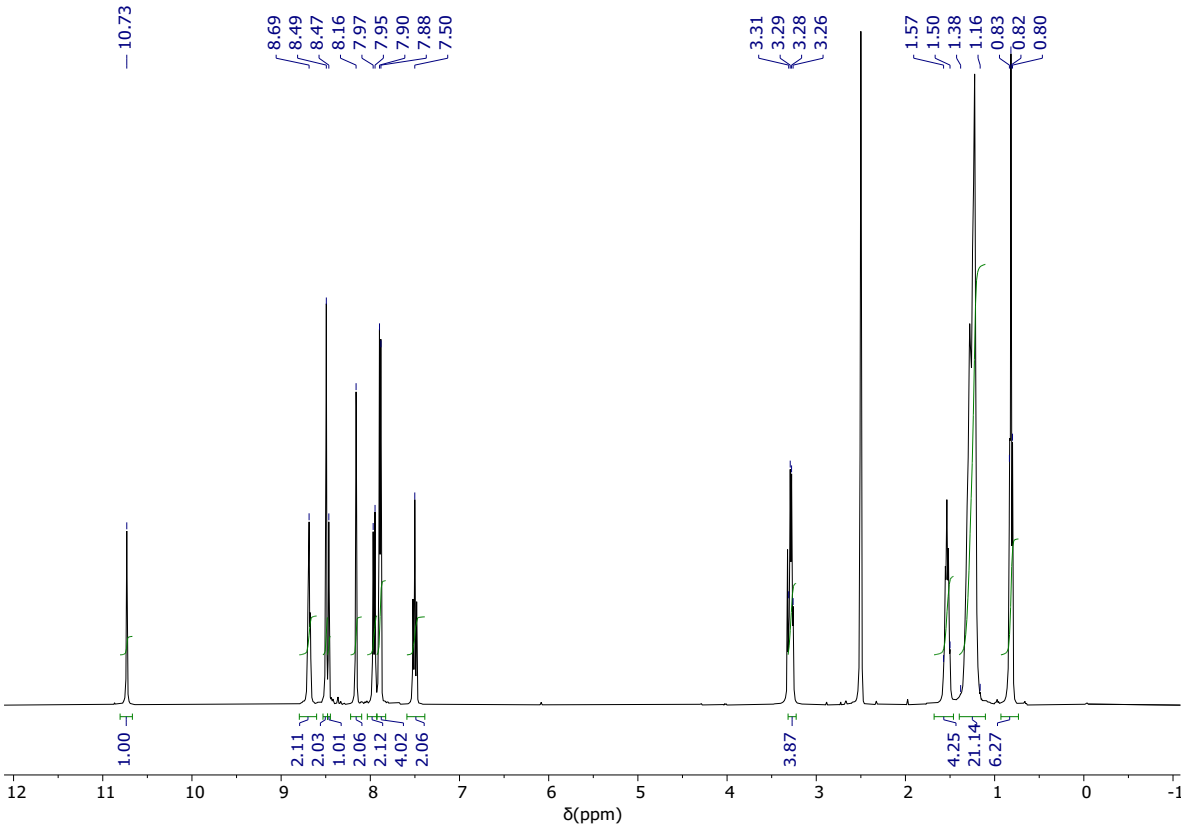

$^{31}P\{^{1}H\}$ NMR (DMSO-d_6)

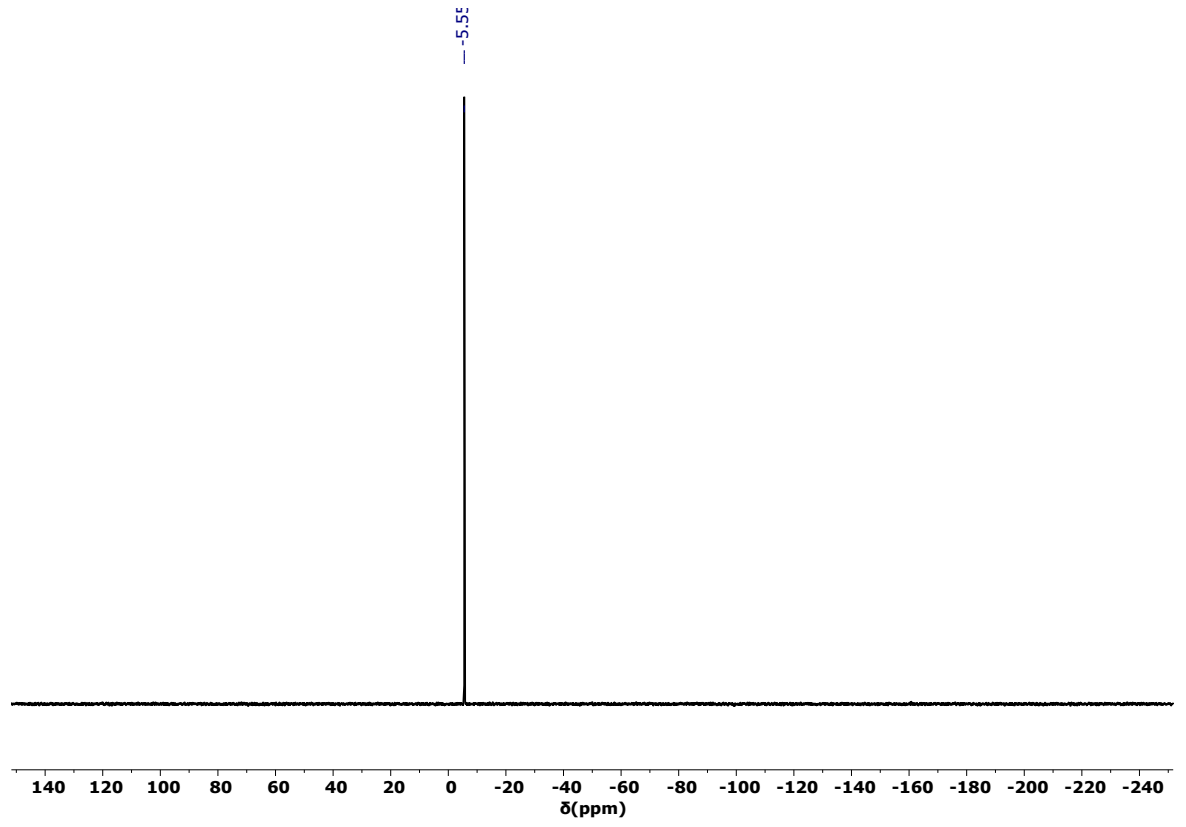

$^{19}F\{^{1}H\}$ NMR (DMSO-d_6)

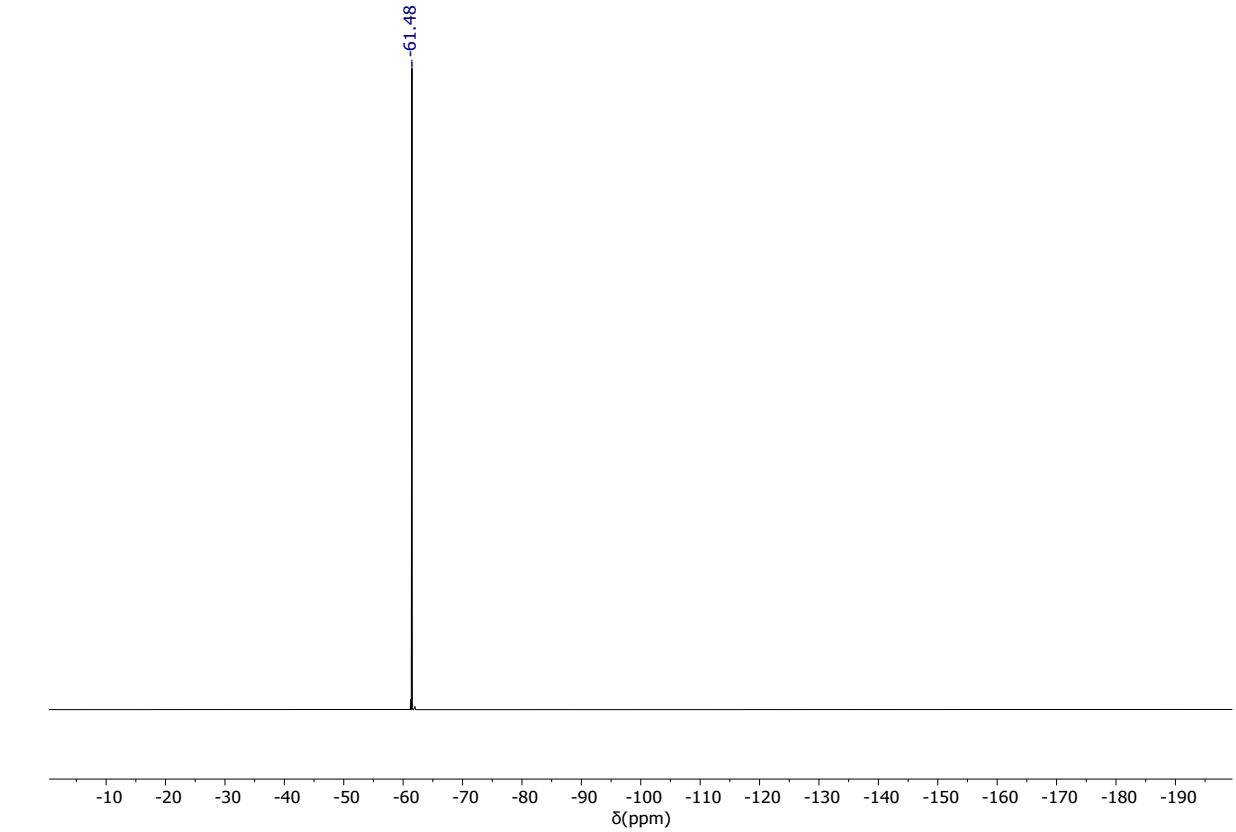

$^{13}C\{^{1}H\}$ NMR (DMSO-d_6) DEPT135

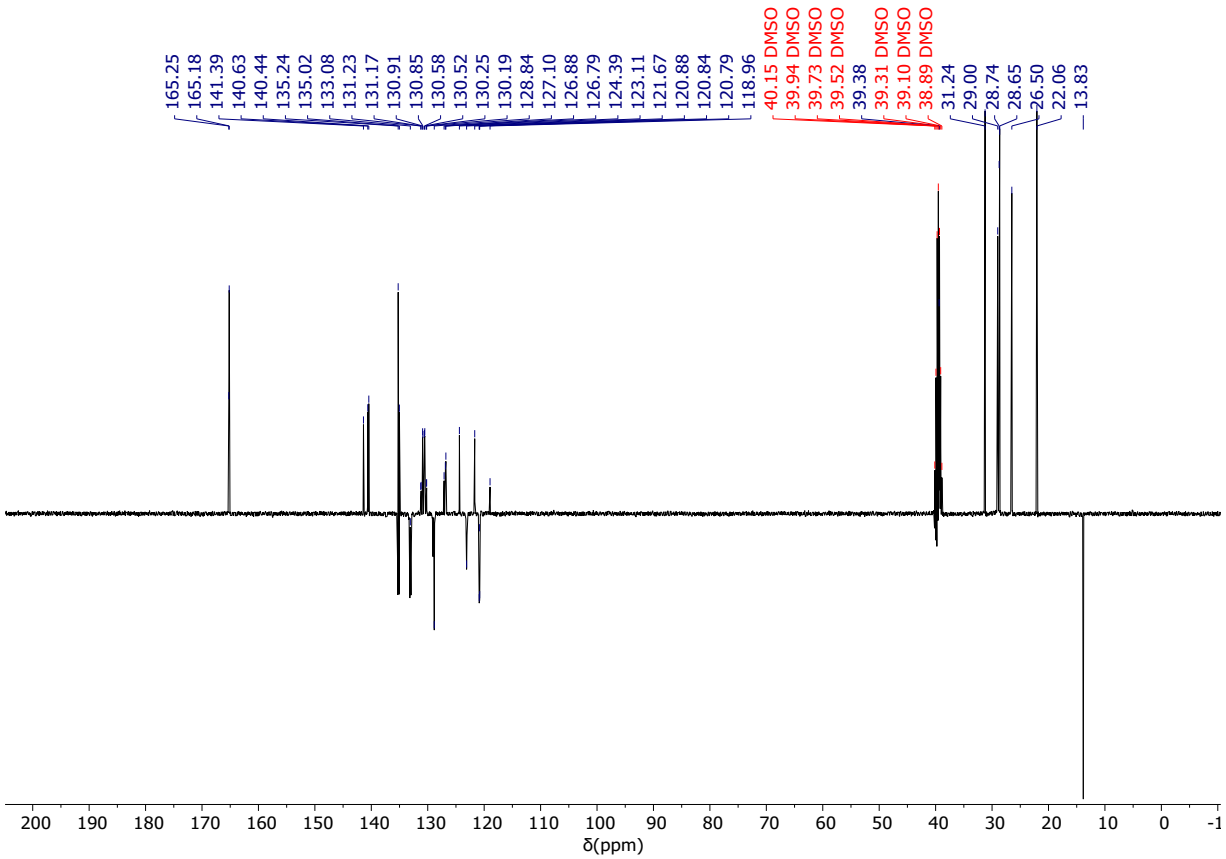

References

1 X. Caumes, A. Baldi, G. Gontard, P. Brocorens, R. Lazzaroni, N. Vanthuyne, C. Troufflard, M. Raynal and L. Bouteiller, *Chem Commun*, 2016, **52**, 13369–13372.

2 A. Desmarchelier, M. Raynal, P. Brocorens, N. Vanthuyne and L. Bouteiller, *Chem Commun*, 2015, **51**, 7397–7400.

3 S. Allenmark, *Chirality*, 2003, **15**, 409–422.

4 J. M. Zimbron, X. Caumes, Y. Li, C. M. Thomas, M. Raynal and L. Bouteiller, *Angew. Chem. Int. Ed.*, 2017, **56**, 14016–14019.

5 Y. Miki, K. Hirano, T. Satoh and M. Miura, *Angew. Chem. Int. Ed.*, 2013, **52**, 10830–10834.

6 J. S. Bandar, M. T. Pirnot and S. L. Buchwald, *J. Am. Chem. Soc.*, 2015, **137**, 14812–14818.

7 M. A. Martínez-Aguirre, Y. Li, N. Vanthuyne, L. Bouteiller and M. Raynal, *Angew. Chem. Int. Ed.*, 2021, **60**, 4183–4191.

8 Y. Li, A. Hammoud, L. Bouteiller and M. Raynal, *J. Am. Chem. Soc.*, 2020, **142**, 5676–5688.

9 D. Niu and S. L. Buchwald, *J. Am. Chem. Soc.*, 2015, **137**, 9716–9721.

10 A. Desmarchelier, X. Caumes, M. Raynal, A. Vidal-Ferran, P. W. N. M. van Leeuwen and L. Bouteiller, *J. Am. Chem. Soc.*, 2016, **138**, 4908–4916.

11 Y. Li, X. Caumes, M. Raynal and L. Bouteiller, *Chem. Commun.*, 2019, **55**, 2162–2165.

12 J. Roosma, T. Mes, P. Leclère, A. R. A. Palmans and E. W. Meijer, *J. Am. Chem. Soc.*, 2008, **130**, 1120–1121.

13 J. D. Roberts and F. J. Weigert, *J. Am. Chem. Soc.*, 1971, **93**, 2361–2369.